UNIVERZITA KARLOVA V PRAZE

Přírodovědecká fakulta

Katedra fyziologie

Bc. Lenka Harantová

OBJEMOVĚ REGULOVANÉ ANIONTOVÉ KANÁLY U ASTROCYTŮ- ANALÝZA *IN VITRO* A *IN SITU*

VOLUME-REGULATED ANION CHANNELS IN ASTROCYTES- *IN VITRO* AND *IN SITU* ANALYSIS

Diplomová práce

Vedoucí diplomové práce: Ing. Miroslava Anděrová, CSc.

Praha 2012

Prohlášení

Prohlašuji, že jsem závěrečnou práci zpracovala samostatně a že jsem uvedla všechny použité informační zdroje a literaturu. Tato práce ani její podstatná část nebyla předložena k získání jiného nebo stejného akademického titulu.

V Praze dne 27.8.2012

Bc. Lenka Harantová

Poděkování

Ráda bych na tomto místě poděkovala své školitelce Ing. Miroslavě Anděrové, Csc. za odborné vedení, trpělivost a shovívavost. Dále bych chtěla poděkovat MUDr. Heleně Pivoňkové, Ph.D. za cenné rady a pomoc při práci v laboratoři.

ABSTRACT

Astrocytes need to preserve constant volume in the face of osmolarity perturbations to function properly. To regain their original volume after hyposmotically induced swelling, they extrude intracellular electrolytes and organic osmolytes, such as inorganic ions, excitative amino acids or polyols, accompanied by osmotically driven water. This process is termed regulatory volume decrease and is ensured by various ion channels and transporters. Recently, much attention has been focused on the ubiquitous volume-regulated anion channels activated by cell swelling. VRACs are moderately outwardly rectifying with intermediary conductance, permeable to inorganic anions and organic osmolytes and sensitive to broad-spectrum anion channels blockers.

Using patch-clamp technique we aimed to characterize VRACs in cultured cortical astrocytes isolated from neonatal Wistar rats and to elucidate the effect of intracellular Na^+ on VRAC activity. In addition, we also intended to characterize these channels *in situ* in brain slices of 10 – 12 days old rats, focusing mainly on hippocampal astrocytes. To induce astrocytic swelling, we exposed astrocytes to hypotonic solution (250 mOsm). In agreement with previous findings, we showed that cultured cortical astrocytes activate VRAC currents upon exposure to hypotonic stress, which are inhibited by DCPIB, a specific VRAC blocker. Moreover, we found that VRAC activity *in vitro* is strongly dependent on intracellular Na^+ – 50 mM Na^+ completely abolished it. *In situ* we were able to detect VRAC activity in a small subpopulation of recorded astrocytes. The observed current was sensitive to DCPIB and tamoxifen.

In summary, elucidating functional properties of VRACs in astrocytes *in situ* is particularly interesting, because many brain pathologies, such as ischemia, traumatic brain injury or hyponatremia, are associated with marked astrocytic swelling and VRACs could thus constitute a target for therapy of cerebral edema.

Key words: cell volume regulation, volume-regulated anion channels, astrocytes, brain edema

TABLE OF CONTENTS

LIST OF ABBREVIATION

AQP4	aquaporin 4
ATP	adenosine 5´-triphosphate
AVD	apoptotic volume decrease
C_m	membrane capacitance
CaM	calmodulin
CaMII	Ca^{2+}/calmodulin-dependent protein kinase II
ClC-3	voltage-gated Cl^- channel
CNS	central nervous system
DCPIB	4-(2-butyl-6,7-dichloro-2-cyclopentylindan-1-on-5-yl) oxybutyric acid
DIDS	4´-diisothiocyanatostilbene-2,2´-disulfonic acid
DNA	deoxyribonucleic acid
EAA	excitatory amino acid
ER	endoplasmic reticulum
ERK	extracellular signal-regulated kinase
FAK	focal adhesion kinase
GluR	glutamate receptor
GODE	gradual osmolarity decrease
GPCR	G-protein coupled receptor
GTPγS	guanosine 5´-[γ-thio]triphosphate
IP_3	inositol 1,4,5-triphosphate
IVR	isovolumetric volume regulation
JNK	c-Jun N-terminal kinase
K_{IR}	inwardly rectifying K^+ channel
MAPK	mitogen activated protein kinase
MDR1	multidrug resistance-1 gene
MEK	MAP kinase kinase
MLCK	myosin-light-chain kinase
mRNA	messenger ribonucleic acid
MRP	multidrug resistance protein
NPPB	5-nitro-1-(3-phenylpropylamino) benzoic acid

PAR	proteinase activated receptor
P-gp	P-glycoprotein
pICln	putative Cl^- channel
PKC	protein kinase C
PLC	phospholipase C
R_I	input resistance
RhoK	Rho-kinase
rMCAO	rat middle cerebral artery occlusion
ROS	reactive oxygen species
RTK	receptor tyrosine kinase
RVD	regulatory volume decrease
RVI	regulatory volume increase
SODE	sudden osmolarity decrease
SON	supraoptic nucleus
Tx	tamoxifen
Tau	taurine
TK	tyrosine kinase
TRPV4	transient receptor potential vanilloid channel 4
V_m	resting membrane potential
VDAC	voltage-dependent anion channel
VRAC	volume-regulated anion channel
VSOAC	volume-sensitive organic osmolyte/anion channel
VSOR	volume-sensitive outwardly rectifying Cl- channel

INTRODUCTION

Astrocytes, the predominant cell type in the central nervous system (CNS), are the cells mainly involved in brain volume homeostasis (Kimelberg 2005). Astrocytes *in vivo* posess a variety of potassium (K^+) and chloride (Cl^-) ion channels that differently contribute to cell volume regulation (Benesova et al. 2012). There is clear evidence that astrocytes swell as a result of ischemia and oxygen glucose deprivation and release high amount of excitatory amino acids (Phillis et al. 2003). These processes play a pivotal role in the pathogenetic mechanisms of the ischemic damage (Kimelberg et al. 2004) and a great effort is currently made to identify the underlying molecular mechanisms. Probably the best described anion channels involved in cell volume regulation are volume-regulated anion channels (VRACs). VRACs, activated by cell swelling, were described in most animal cell types, including astrocytes and it is argued that they play both beneficial and detrimental role during CNS insults – their activation allow astrocytes to regulate their volume, yet in the same time, they contribute to the excitotoxic damage of brain tissue.

The aim of this thesis is electrophysiological characterization of VRACs in astrocytes *in vitro* and *in situ.*

ASTROCYTES

1.1 Basic characteristics

Parenchyma of the mammalian central nervous system (CNS) is composed of neuroepithelial cells, neurons and glial cells. The latter group comprises oligodendrocytes, NG2-glia, microglia and astrocytes. Glial cells, except for microglia, are of ectodermal origin and their number in human brain roughly equals that of neurons (Azevedo et al. 2009). Astrocytes are the most abundant of neuroglial cells and can occupy up to 30% of brain volume, depending on the brain region (Kimelberg 2005). The former, classical, view has seen astrocytes as passive cells serving mainly as a connective tissue. However, in the light of recent findings it becomes increasingly evident that astrocytes actively participate in virtually all processes in the CNS.

Astrocytes are star-like cells extending few primary processes, further branching into fine secondary processes, often described as spongiform. Endings of astrocytic processes are in direct contact with the pial surface, blood vessels or they enwrap synapses (Verkhratsky et el. 2007). Figure 1 illustrates typical astrocytic morphology.

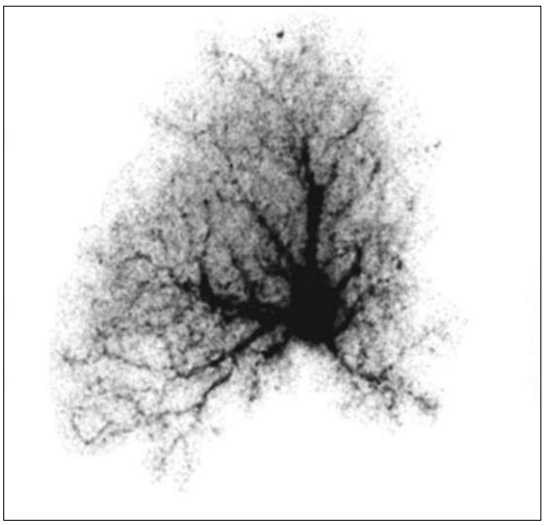

Figure 1. Protoplasmic astrocyte with highly ramified processes (Wilhelmsson et al. 2006)

Two types of astrocytes are usually distinguished based on studies in rodent brain – protoplasmic and fibrous astrocytes. Protoplasmic astrocytes are typically found in grey matter and possess thick, highly branched processes, whereas fibrous astrocytes reside predominantly in white matter and have fewer thin processes with less prominent branching. Other cells with astrocytic properties are Bergmann glia of the molecular layer of the

cerebellum, and the Muller cells of the retina. Astrocytic properties, e.g. their number and morphology, alter during phylogenesis. Human protoplasmic astrocytes are larger and extend greater number of longer, thicker and more elaborate processes than their rodent counterparts. In addition, two more types of astroglia have been described in human brain – interlaminar and varicose projection astrocytes (Oberheim et al. 2009). Astrocytes in culture and *in vivo* interlink via gap junctions into functional syncytia allowing for intercellular communication and trafficking (Schools et al. 2006). Gap-junctional coupling *in vivo* occurs at the ends of astrocytic processes (endfeet), while astrocytic bodies are organized in neuropil in such manner, that every astrocyte occupies separate area. This area contains synapses and blood vessels in contact with the astrocyte – thus every astrocyte controls distinct anatomical microdomain (Bushong et al. 2002). Astrocytic organization into microdomains is illustrated in Figure 2.

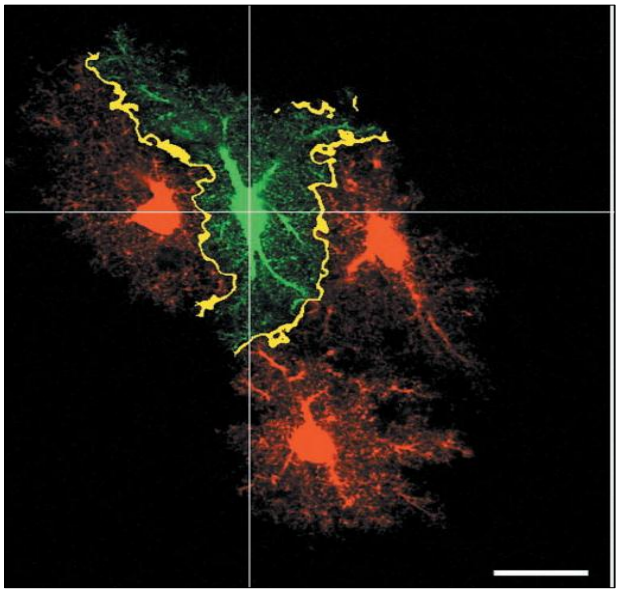

Figure 2. Astrocytic microdomains and colocalization between adjacent astrocytes. Astrocytes are labeled with fluorescent dye Alexa Fluor 488 and 568. Area of interaction is depicted in yellow (Bushong et al. 2002)

Commonly used marker for immunocytochemical identification of astrocytes is glial fibrilary acidic protein (GFAP), an intermediate filament protein specifically expressed in the CNS by astrocytes (Bushong et al. 2002). However, recent studies suggest that there is a population of GFAP-negative astrocytes (Walz et al. 1998; Cahoy et al. 2008) and identification of astrocytes based on GFAP-immunostaining can yield misleading results. Glutamate aspartate transporter (GLAST, Schools et al. 2006) or aldehyde dehydrogenase 1 family member L1 (Aldh1L1) are alternative and perhaps more accurate astrocyte-specific markers; in addition, Aldh1L1 immunostaning allows a better visualization of highly branched astrocytic

morphology than GFAP, which delineates only approximately 15% of total astrocytic volume and its expression is confined predominantly to astrocytic somata and main processes, whereas only little GFAP is found in the fine spongiform processes (Bushong et al. 2002; Cahoy et al. 2008).

1.2 Membrane properties

Astroglial cells are characterized by low membrane resistance (30 – 150 MΩ) and negative resting membrane potential (approximately -80 mV). However, electrophysiological properties of astrocytes change during brain maturation. Three populations of astrocytes with different currents profiles can be found in developing rodent CNS – outwardly rectifying astrocytes (ORA), variably rectifying astrocytes (VRA) and passive astrocytes (PA) (Schools et al. 2006). ORA display depolarization-induced inwardly rectifying Na^+ currents, transient outwardly rectifying K^+ currents (K_A) and delayed outwardly rectifying K^+ currents (K_{DR}). VRA express both inwardly and outwardly rectifying K^+ currents. PA are characterized by non-decaying, time- and voltage-independent K^+ currents, further termed passive currents. These currents exhibit linear current-voltage relationship. It was shown that ORA, VRA and PA represent subsequent stages of development of astroglial cells. Numbers of ORA and VRA gradually decrease during postnatal ontogenesis, 90% of astrocytes in the hippocampus of adult animals display passive currents pattern (Zhou et al. 2006). Representative current profiles for each electrophysiological phenotype are depicted in Figure 3. Passive conductance is mediated mainly by TWIK-1 and TREK-1 channels belonging to the two-pore-domain potassium channel family (Zhou et al. 2009) and to some extent, also by interastrocytic gap junctions (Schools et al. 2006).

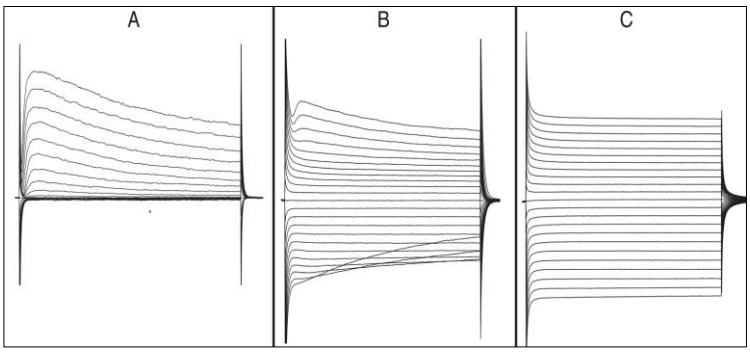

Figure 3. Representative current profiles of ORA (A), VRA (B) and PA (C) (Schools et al. 2006)

1.3 Function

Astroglia fulfill a plethora of functions – they provide guidance and support to migrating neurons during CNS development, participate in blood-brain barrier formation and maintenance, regulate cerebral microcirculation and energetically support neurons and, most importantly, regulate the homeostasis of CNS microenvironment and synaptic transmission (Verkhratsky et al. 2007).

1.3.1 Ion homeostasis

The ionic/neurotransmitter homeostasis of CNS extracellular space (ECS) must be tightly controlled in order to ensure proper brain function.

K^+ homeostasis. Neuronal activity results in increased concentration of extracellular K^+, which could compromise neurotransmission – elevated K^+ depolarizes neuronal membranes, which could increase neuronal excitability by bringing their membrane potential closer to action potential threshold, or conversely cause neuronal inexcitability, if the neuronal depolarization was high enough for Na^+ channels to become inactivated (Verkhratsky et al. 2007). One of the processes ensuring extracellular K^+ homeostasis is astrocytic spatial buffering schematically depicted in Figure 4. Astrocytic resting membrane potential (V_m) is close to the equilibrium potential for K^+ and increased $[K^+]_o$ leads to net K^+ uptake into surrounding astrocytes. K^+ is then redistributed throughout astrocytic syncytium and to the perivascular areas, where $[K^+]_o$ is lower and electrochemical gradient of K^+ favours its release. Inward and outward K^+ movements in astrocytes are mediated predominantly by inwardly rectifying K^+ channel ($K_{IR,}$ Butt et al. 2006). Subcellular localization of K_{IR} channels reflects their role in K^+ clearance – K_{IR} expression is enriched in perisynaptic portions of astrocytic membranes and in the endfeet contacting blood vessels (Higashi et al. 2001). To maintain electrochemical neutrality, K^+ is accompanied by Cl^-, passing through specific anion channels and Cl^- transporters. However, according to some studies, K_{IR} play only a minor role in K^+ clearance during neuronal firing and K^+ uptake is mediated predominantly by Na^+/K^+-ATPases (D´Ambrosio et al. 2002).

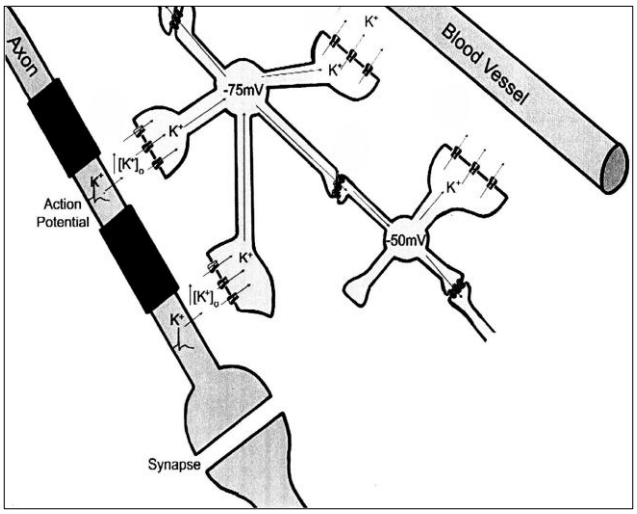

Figure 4. Schematic depiction of spatial K^+ buffering by astrocytes. Extracellular K^+ is absorbed by astrocytes via inwardly rectifying K^+ channels (K_{IR}) and redistributed through astrocytic syncytium to areas with low K^+ concentration, where it is released. (Butt et al. 2006).

Na^+ homeostasis. Resting Na^+ concentration in astrocytes is approximately 15 mM (Rose et al.1996) and maintenance of Na^+ gradient is necessary for the proper function of Na^+/K^+-ATPase and Na^+-dependent transport systems. Astrocytic Na^+ levels increase in response to various stimuli, such as neuronal activity or transport processes. During neuronal firing, Na^+ released by neurons enters perisynaptic astrocytes through the action of Na^+/K^+-ATPases and glutamate transporters and receptors (Langer et al. 2009). Increased $[Na^+]_i$ stimulates $Na^{+/}K^+$-ATPase, ATP consumption and glucose uptake and metabolism. Glucose is metabolized to lactate, which serve as a fuel to neurons (Simard et al. 2004). Glutamate-evoked Na^+ elevations spread through the astrocytic syncytium (similarly to Ca^{2+} waves described below), thus coupling glial metabolism with neuronal activity (Loaiza et al. 2003).

1.3.2 Neurotransmitter homeostasis

Another consequence of neuronal firing is increased extracellular concentration of neurotransmitters. These neuroactive substances must be removed from synaptic cleft in order to ensure proper neurotransmission. It can be achieved by their decomposition as in the case of acetylcholine or by their reuptake. Synapses are in close contact with processes of neighbouring astrocytes, populated by a wide range of neurotransmitter receptors and transporters (Hansson et al. 2003). Perisynaptic localization and expression of proteins for neurotransmitter detection and transport allows astrocytes to control synaptic environment and maintain its homeostasis and thus functionality. The main excitatory neurotransmitter in mammalian brain is L-glutamate. However, it is a potent neurotoxin at the same time and prolonged overstimulation of neuronal glutamate receptors leads to excitotoxic neuronal

death; therefore extracellular glutamate levels must be kept low. Astrocytes express high affinity glutamate transporters GLAST1 and GLT1, transporting one glutamate (or aspartate) molecule together with three Na^+ (or two Na^+ and one H^+) in exchange for one K^+ and one OH^- (or one HCO_3^-) (Simard et al. 2004). Glutamate in astrocytes is then converted to glutamine via the glutamine synthetase pathway: Glutamate + NH_3 + ATP → Glutamine + ADP + P_i. Glutamine is released back to ECS and taken up by neurons, where it is hydrolysed to glutamate and ammonia by mitochondrial phosphate-dependent glutaminase: Glutamine → Glutamate + NH_3.

1.3.3 Gliotransmission

Astrocytes have been considered to be electrically non-excitable cells. However, evidence has been accumulating that astrocytes sense neuronal activity and react to it with Ca^{2+} oscillations. Moreover, they can actively modulate neurotransmission. These findings led to the development of the concept of tripartite synapse in late 1990s. This model suggests that chemical synapse is formed by three elements – presynaptic and postsynaptic terminals and perisynaptic astrocyte. Astrocytes do not only sense neuronal activity, but they are able to discriminate between different neurotransmitters used by different synapses and selectively react to specific neuronal pathway (Perea et al. 2005; Schipke et al. 2008). When stimulated simultaneously by different neurotransmitters, astrocytic Ca^{2+} signaling is non-linearly modulated depending on the level of synaptic activity (Perea et al. 2005). Stimulation of astrocytic receptors with neurotransmitters induces elevation of intracellular Ca^{2+}, which originates mainly from inositol 1,4,5-triphosphate-sensitive Ca^{2+} stores. Ca^{2+} waves, elicited by neurotransmitter exposure, move through astrocytic syncytium, providing extra-neuronal pathway for signal propagation. As a reaction to Ca^{2+} oscillation, astrocytes release neuroactive substances, termed gliotransmitters because of their glial origin, such as glutamate and purines, in a process called gliotransmission, and thus modulate excitability of adjacent neurons (Perea et al. 2009). Gliotransmitter release is mediated by one or more of following mechanisms: Ca^{2+}-dependent exocytosis, reversal of glutamate transporters, volume-regulated anion channels, glutamate exchange via the cystine–glutamate antiporter, release through ionotropic purinergic receptors or hemichannels (Malarkey et al. 2008). Astrocytic Ca^{2+} waves can occur spontaneously. According to Bonansco and co-authors (2011), spontaneous Ca^{2+} oscillations and subsequent efflux of gliotransmitters are important for setting the basal probability of synaptic neurotransmitter release and modify the threshold for long term potentiation induction.

Taken together, astrocytes play an important role in synaptic information processing, integration and transmission and influence synaptic plasticity. However, not all synapses are tripartite – in the CA1 area of rat hippocampus, only approximately 60% of synapses are contacted by the processes of perisynaptic astrocytes (Ventura et al. 1999).

2. PATCH-CLAMP

The patch-clamp technique was developed in early 1980s by Bert Sakmann and Erwin Neher to measure currents through muscle nicotinic acetylcholine receptors. The method underwent many refinements since then and became invaluable tool for neuroscience. The method consists in electrical isolation of tiny patch of membrane, which allows to record currents flowing through the patch. It is achieved by sucking the membrane inside a tip of a glass pipette filled with appropriate electrolyte solution, which results in a formation of a high resistance (in the range of GΩ) seal. Several basic configurations are routinely employed depending on the aim of the experiment and they are summarized in Figure 5. During classic whole-cell recording, soluble cytoplasmic elements are diluted or washed out by the pipette fluid. To preserve more or less physiological intracellular milieu while having electrical access to the cytoplasm, perforated patch-clamp was developed. The principle of perforated patch-clamp relies on the action of pore-forming compounds, such as nystatin or amphotericin B, creating holes in membranes permeable to ions but not larger molecules (Molleman 2003). Patch-clamp method provides assessment of active and passive electrical properties of cellular membranes and allows electrophysiological characterization of ion channels and transporters.

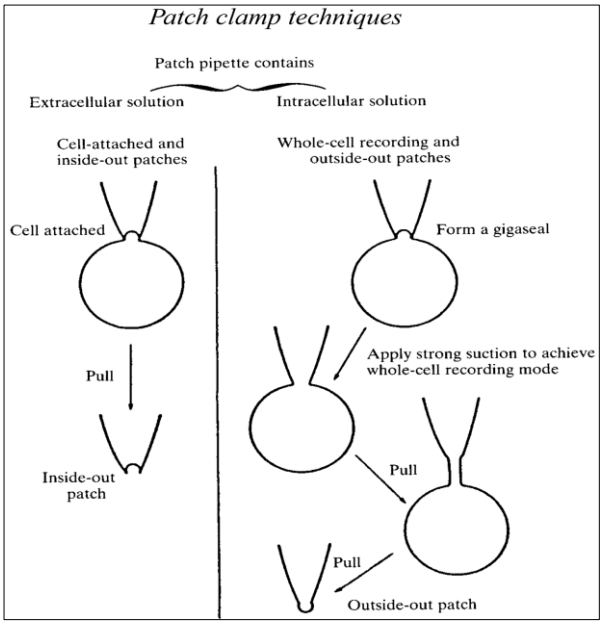

Figure 5. Patch-clamp configurations
Cell-attached – when the pipette is in closest proximity to the cell membrane, mild suction is applied to gain a tight seal between the pipette and the membrane. *Whole-cell* – by applying brief suction, the cell membrane is ruptured and the pipette gains access to the cytoplasm. *Inside-out* – in the cell-attached mode, the pipette is retracted and the patch is separated from the membrane and exposed to air; the cytosolic surface of the membrane is exposed. *Outside-out* – in the whole-cell mode, the pipette retraction results in vesicular structure with the cytosolic side facing the pipette solution. (Ogden 1994)

3. VOLUME-REGULATED ANION CHANNELS

3.2 Basic properties

Volume-regulated anion channels (VRAC) are also known as volume-sensitive organic osmolyte/anion channels (VSOAC; Jackson et al. 1995) or volume-sensitive outwardly rectifying Cl^- channels (VSOR; Okada 1997). They are found in virtually all animal cell types and as their name suggests, they play a role in cell volume regulation. Over the past twenty years, VRACs have been extensively studied in different animal cell types – e.g. in endothelial cells (Nilius et al. 2000), neurons (Pasantes-Morales et al. 1993) and astrocytes (Pasantes-Morales et al. 1994); however, there are many questions that remain to be answered. The most important question is whether the perceived features attributed to VRACs are a manifestation of one type of ion channels or rather a combined behaviour of a group of channels.

VRACs are ubiquitous ion channels permeable to inorganic and organic anions (represented in the CNS predominantly by chloride and glutamate, respectively) as well as to various organic osmolytes such as taurine or polyols (Okada 1997) and possibly to adenosine-5'-triphosphate (ATP; Hisadome et al. 2002). Their anion permeability sequence is $NO^- > I^- > Br^- > Cl^- > F^-$ > gluconate, they are outwardly rectifying and inactivate at potentials more positive than 50 mV (Jackson et al. 1995). The diameter of the channel pore was estimated to be 0.6 – 0.7 nm (Ternovsky et al. 2004). VRACs are inhibited by broad spectrum chloride channel blockers DIDS (4,4'-diisothiocyanatostilbene-2,2'-disulfonic acid; Estevez et al. 1999), NPPB (5-nitro-1-(3-phenylpropylamino) benzoic acid; Phillis et al. 1997), tamoxifen (Phillis et al. 1998) and selective serotonin reuptake inhibitors, such as fluoxetine, sertraline and paroxetin (Maertens et al. 2002). The most selective blocker of VRACs reported so far is a derivative of ethacrynic acid, DCPIB (4-(2-butyl-6,7-dichloro-2-cyclopentylindan-1-on-5-yl)oxybutyric acid; Decher et al. 2001). VRACs are also inhibited in voltage-dependent manner by extracellular ATP in concentration $\geq$ 10 mM acting as an open channel blocker (Jackson et al. 1995).

3.3 Activation

As their name suggest, VRACs are activated in response to the cell swelling, that is, as a result of the cell volume expansion. Cells must be therefore capable of sensing alterations of their volume and transduce them, among other actions, into VRAC opening.

Widely used experimental model of cell swelling is exposing the cells to the hypotonic stress. VRACs are activated when the relative cellular surface area increases by approximately 25% (Okada 1997) and their opening is probably not due to the membrane stretch, because there is a lag period of 5 – 10 s between cell swelling and the appearance of VRAC currents (Kubo et al. 1992). Intracellular ATP is necessary for sustained VRAC activation (Rutledge et al. 1999), which might require phosphorylation of some yet unidentified accessory protein or the channel itself (Crepel et al. 1998) or non-hydrolytic ATP binding (Jackson et al. 1994). Following events occurring during hypotonic stress-induced cell swelling have been proposed to initially trigger VRAC activation: reduction of intracellular ionic strength, alterations of cytoskeleton organization and changes in intracellular calcium concentration.

Cell swelling leads to a dilution of the intracellular milieu and thus to a reduction of ionic strength due to an increase of cell water content and increased efflux of ions, mainly K^+ and Cl^-, which is discussed in the section on regulatory volume decrease (RVD). Alterations in ionic strength could affect VRAC directly or via molecules involved in signaling pathway regulating VRAC opening by changing their surface potential (Okada et al. 2009). Decreased intracellular ionic strength triggers VRAC activation in endothelial cells (Schliess et al. 1996), whereas it has merely modulatory effect on VRAC activation in chinese hamster ovary cells (Cannon et al. 1998) and C6 glioma cells (Emma et al. 1997), where it seems to decrease volume set point for the channel opening. Another effect of cell swelling is a reorganization of cellular cytoskeleton, notably of the F-actin (stress fibers; Moran et al. 1996). Actin cystoskeleton is essential for cell shape determination and motility and it affects various membrane transporters. In cultured astrocytes with typical polygonal flat morphology, it was possible to elicit Cl^- currents resembling VRAC currents by cytochalasin-induced actin disruption in the absence of cell swelling (Lascola et al. 1996). Furthermore, functional Rho/Rho kinase/myosin light-chain phosphorylation pathway regulating the stress fiber formation is necessary for full VRAC activation in vascular endothelial cells (Nilius et al. 2000; Carton et al. 2002). The role of intracellular Ca^{2+} is discussed in the next section.

3.4 Modulation

While the activation mechanism remains rather elusive, modulation of the channel is quite well understood. Agents exerting important modulatory effect on VRAC functioning are extracellular ATP, calcium and protein kinases.

ATP. One of the initial cellular reaction to swelling is ATP release. ATP can then mediate intercellular communication – it serves as a gliotransmitter and regulates astrocytic

calcium signaling (Koizumi 2010). During hypotonicity-induced swelling, there is an increased ATP efflux from astrocytes, possibly via multidrug restistance-associated protein (MRP; Darby et al. 2003) or maxi-anion channels (Liu et al. 2008); this ATP then upregulates osmotically activated VRACs through a calcium-dependent mechanism (Mongin et al. 2002) discussed in detail in the next section. In hepatoma cells, ATP released in reaction to swelling is necessary for full VRAC activation; it acts in autocrine manner on purinergic P2 receptors and couples cell volume alterations with VRAC opening (Wang et al. 1996). Interestingly, knockdown of AQP4 with small interfering RNA (siRNA) downregulates VRACs in cultured astrocytes, but this effect can be reversed by increasing intracelllular ATP (Benfenati et al. 2007).

Calcium. Another event typically observed as a reaction to cell swelling is a rise in intracellular calcium concentration ($[Ca^{2+}]_i$). Astrocytes, as well as other cell types, exposed to hypotonic stress display transient increase of intracellular calcium followed by a drop of $[Ca^{2+}]_i$ to a sustained plateau concentration, which remains higher than the resting level. The calcium enters the cytosol from both intracellular stores and extracellular space (Schliess et al. 1996). The influx of extracellular Ca^{2+} is mediated, at least in part, by transient receptor potential vanilloid channel 4 (TRPV4). TRPV4 is weakly Ca^{2+} selective cationic channel localized mainly in astrocytic endfeet contacting pial surface and brain vasculature. TRPV4 is activated in response to hypotonic stimuli (Benfenati et al. 2007) and its ablation results in abnormal osmosensing and osmoregulation in mice (Mizuno et al. 2003). The calcium transients, being a common feature of cell swelling in different animal cell types, make calcium a plausible candidate for the initial signal transducing cell volume increase into VRAC activation (Morales-Mulia et al. 1998). However, VRACs in most cell types seem to be calcium-independent (Pasantes-Morales et al. 2000) although according to Mongin and colleagues, they require submicromolar $[Ca^{2+}]_i$ to function properly in astrocytes (Mongin et al. 1999). Calcium further modulates VRAC activity as an effector of some protein kinase signaling pathways.

Protein kinases. Protein kinases can be divided into two groups – tyrosine kinases (TK) and serine/threonine protein kinases, depending on the amino acid residue they phosphorylate. Tyrosine kinases participate in signaling pathways regulating various cellular functions, such as cell motility, proliferation, differentiation or survival. We can distinguish receptor and non-receptor TKs, and members of both groups were shown to become activated in response to hypotonic stress (Pasantes-Morales et al. 2006). Several studies have shown, that VRAC activity is promoted by TKs, some of which are, as a matter of fact, activated in

response to cell swelling. Inhibiting of TKs with genistein or herbimycin A results in substantial decrease in osmotically induced VRAC currents in human Intestine 407 cells (Tilly et al. 1993), cultured astrocytes (Crepel et al. 1998) and *in vivo* in ischemic/reperfused rat brain (Phillis et al. 1996), whereas blocking of protein tyrosine phosphatase potentiates VRAC currents, at least in human Intestine 407 cells (Tilly et al. 1993). Specific TKs and signaling pathways are not known; however, Src-family kinases are involved in VRAC modulation in B lymphocytes, where p56lck mediates osmotically induced channel opening (Lepple-Wienhues et al. 1998) and in cultured astrocytes, where peroxynitrite ($ONOO^-$) increases VRAC activity via Src-kinase pathway (Haskew et al. 2002; Kimelberg 2004). It is noteworthy that Src-kinases modulate hyposmoticaly activated TRPV4 as well (Wegierski et al. 2009). VRACs are also upregulated as a result of epidermal growth factor receptor (EGFR) stimulation (Tilly et al. 1993; Abdullaev et al. 2003). EGFR pathway includes mitogen activated protein kinases (MAPK) belonging to the serine/threonine protein kinase family, namely extracellular signal-regulated kinases 1 and 2 (ERK-1, ERK-2). These were shown to have a modulatory effect on VRACs in different cell types. In cultured astrocytes (Crepel et al. 1998) and C6 glioma cells (Belsey et al. 2007), ERKs become activated in response to hyposmolarity and their inhibition significantly downregulates VRAC activity. The hypotonicity-induced increase in ERK-1/2 activity in cultured astrocytes is Ca^{2+}-mediated and requires functional Ras/Raf pathway (Schliess et al. 1996) and TKs (Crepel et al. 1998). In human Intestine 407 cell line, ERK-1/2 also activate in response to hypotonicity, but have no influence on osmotically induced VRAC currents. However, they mediate the VRAC-potentiating effect of ATP; ATP is released into the extracellular space early after the onset of cell swelling and binds to P2Y receptor, triggering signaling events that eventually lead to ERK-1/2 activation and VRAC upregulation (Van der Wijk et al. 1999). Similar ATP action have been observed in astrocytes and following signaling pathway has been suggested: extracellular ATP activates P2Y receptors coupled to phospholipase C (PLC), which results in IP_3 production and subsequently release of Ca^{2+} from IP_3-sensitive intracellular stores. Increased $[Ca^{2+}]_i$, and possibly diacylglycerol, which is another product of PLC-mediated hydrolysis of membrane phospholipids, then may activate protein kinase C (PKC), α and β1 isoforms (Rudkouskaya et al. 2008), which enhances VRACs. It is noteworthy, that tamoxifen, a potent VRAC blocker, is also an inhibitor of PKC (Horgan et al. 1986). Another consequence of cytosolic Ca^{2+} rise is an activation of calcium/calmodulin-dependent protein kinase II (CaMKII) contributing to the potentiating effect of ATP (Mongin et al. 2005). Central role of Ca^{2+} in VRAC regulation is further supported by following findings: thrombin

increases VRAC activity in Ca^{2+} and PKC dependent manner (Cheema et al. 2005) and hydrogen peroxide (H_2O_2) and ionomycin, a calcium-mobilizing agent, potentiates VRACs via CaMKII pathway (Cardin et al. 2003; Haskew-Layton et al. 2005).

3.5 Physiological and pathophysiological role for VRACs

Determination of physiological, or patophysiological for that matter, role of VRAC is rather difficult because the channel has not been identified on a molecular level. This is mainly due to the fact, that VRACs are expressed in practically all animal cell types and there is no highly specific channel ligand or blocker. However, several proteins have been proposed to represent VRACs, namely P-glycoprotein (P-gp), putative chloride channel (pI_{Cln}) and voltage-gated chloride channel of the ClC-family (ClC3).

P-glycoprotein is a product of the multidrug resistance-1 (MDR1) gene. It belongs to the family of ATP-binding cassette transporters and is responsible for the cell resistance to the neoplastic drugs. It was suggested, that P-gp could act as both transporter and swelling-activated Cl^- channel (Valverde et al. 1992), but this hypothesis was later rebutted by the findings that antisense oligonucleotides inhibiting P-gp expression, antibodies against P-gp or verapamil (a P-gp blocker), did not affect VRAC currents (Tominaga et al. 1995). Another suggested protein, pI_{Cln}, resembles VRACs by its outward rectification, blockage by extracellular nucleotides and inactivation at positive potentials. However, it is localized to the cytoplasm rather than to the cell membrane (Emma et al. 1998), and pI_{Cln} currents differs from VRAC currents in rectification pattern, anion-selectivity, pharmacology and kinetics (Voets et al. 1996). ClC-3 channel belongs to the ClC voltage-gated chloride channel family and similarly to VRAC, it is activated by cell swelling, sensitive to tamoxifen and DIDS and displays a permeability sequence unusual for ClC-family channels – $P_{I^-} > P_{Cl^-}$. Some studies have reported that ClC-3 was a component of VRAC (Hermoso et al. 2002), others, however, found no connection between the two channels (Stobrawa et al. 2001; Abdullaev et al. 2006). Given that there is neither specific ligand nor selective blocker and the channel molecule has not been isolated, putative functions of VRACs have been determined based on how the channel(s) manifest. It is assumed, that their main role is the regulation of cell volume and thus participation in processes involving cell volume alterations, such as regulatory volume decrease (RVD), apoptosis, cellular proliferation and migration, intercellular communication and brain edema formation.

3.5.1 Regulatory volume decrease

Most animal cell types have plasma membranes readily permeable to water and changes in extracellular or intracellular osmolarity are followed by water movement into or out of the cell to maintain the osmotic equilibrium. Net water influx or efflux then causes cell to shrink or swell, respectively. The extracellular surroundings of most cells is fairly constant, yet cell volume homeostasis can be disturbed by basic cellular tasks, such as nutrient uptake, membrane transport or metabolic processes (Okada et al. 2001). Cell volume homeostasis is necessary for proper cell functioning and communication (Pasantes-Morales et al. 2002). To study cell volume regulations, a widely used model is hypotonicity-induced cell swelling. In this experimental setting, cells are exposed to sudden and substantial, routinely up to 30%, decrease in extracellular osmolarity, resulting in cell volume increase. To restore original cell size, intracellular osmolytes are extruded into the extracellular space, followed by osmotically driven water. The released solutes are mainly K^+ and Cl^- ions, amino acids such as aspartate, glutamate and taurine, polyols and other compounds, e. g. creatinine. This process is called regulatory volume decrease (RVD). RVD allows cells to recover 70 – 80% of their original volume within few minutes after the onset of swelling (Pasantes-Morales et al. 2002). Inorganic ions represent 60 – 70 % of released osmolytes, the remaining 30 – 40% are contributed by organic compounds (Massieu et al. 2004). VRACs play essential role in RVD as they mediate flux of Cl^- ions and amino acids aspartate, glutamate and taurine (Pasantes-Morales et al. 1994) and VRAC inhibition also blocks RVD. However, large and sudden osmolarity decrease (SODE) used under experimental conditions is probably never encountered by cells *in vivo*. Extracellular osmolarity *in vivo* is more likely to decrease gradually. Proximal renal tubule cells seem able to continuously adjust and thusly maintain their volume even when extracellular osmolarity is slowly and gradually diminished by 50% (small and gradual osmolarity decrease, GODE). This behaviour was termed isovolumetric volume regulation (IVR), to distinguish it from RVD (Lohr et al. 1986) and it seems to occur, to some extent, also in cultured astrocytes and C6 glioma cells. It has been demonstrated that both cell types exposed to gradually lowered osmolarity (-18 mOsmol/min), swell, but substantially less compared to cells subjected to SODE of the same magnitude (Ordaz et al. 2004; Ordaz et al. 2004). VRACs supposedly could participate in IVR, however their possible contribution has not been explored. RVD mechanism is schematically depicted in Figure 6.

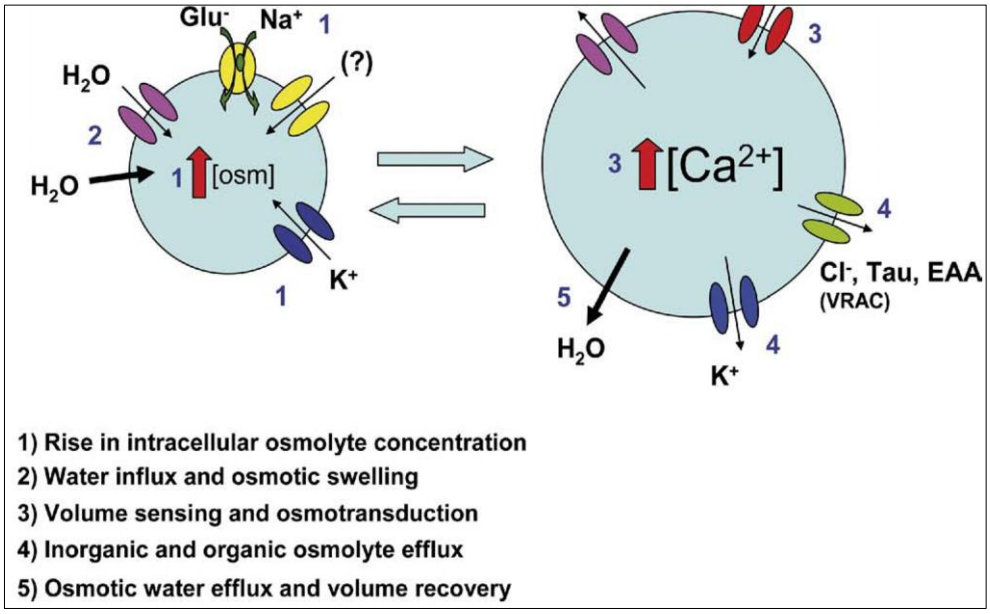

Figure 6. Schematic representation of regulatory volume decrease
1) A rise in intracellular osmolyte concentration via specific ion channels and transporters, 2) Water influx through AQP4 and osmotic swelling, 3) Volume sensing and osmotrasduction, rise in $[Ca^{2+}]_i$, 4) Inorganic and organic osmolyte efflux through appropriate channels, 5) Osmotic water efflux and volume recovery; AQP4 – aquaporin 4, TRPV4 – transient receptor potential vanilloid channel 4, VRAC – volume-regulated anion channel, Tau – taurine, EAA – excitatory amino acids. (Benfenati et al. 2009)

3.5.2 Apoptosis

Apoptosis is a type of programmed cell death, which plays an essential part in embryogenesis, immune system maturation, organ development and cell turnover, as well as in numerous pathological states. During apoptotic process, cellular biochemistry and morphology are altered and following events are typically observed: cell shrinkage, cytochrome c release, activation of caspases, nuclear condensation, DNA laddering and eventually cell fragmentation into apoptotic bodies.

The mechanism of normotonic cell shrinkage occurring at the onset of apoptosis, called apoptotic volume decrease (AVD), is similar to RVD. It is achieved by controlled release of osmolytes, mainly Cl^- and K^+ via separate ion channels and consequent water efflux. In healthy cells, cell shrinking is counteracted by the process of regulatory volume increase (RVI) consisting of the uptake of extracellular osmolytes (mainly Na^+ and Cl^-) accompanied by water influx. In apoptotic cells, RVI is impaired (Maeno et al. 2006). AVD is prerequisite to all other apoptotic events as listed above and its abolition prevents

apoptotic cell death. VRACs involvement in AVD is supported by the fact that AVD, and consequently apoptosis, can be inhibited by VRAC blockers, such as DIDS and NPPB, and RVD is facilitated in cells undergoing AVD (Maeno et al. 2000). VRAC activation during RVD occurs only when cells swell and their volume reaches a certain threshold, yet during AVD they are active in non-swollen or shrunken cells. It is probably due to the shift in the VRAC volume set point to lower levels. The volume set point shift could be mediated by the action of reactive oxygen species (ROS). H_2O_2 positively modulates VRACs in swollen astrocytes, as mentioned above, and other ROS generated during staurosporine-induced apoptosis in HeLa cell culture promote AVD (Shimizu et al. 2004). ROS are also produced during pathophysiological processes *in vivo*, such as ischemia/reperfusion, where they contribute to apoptotic neuronal death (Mongin 2007). The volume set point could be also influenced by intracellular ATP, which is significantly increased in apoptotic cells (Zamaraeva et al. 2005).

3.5.3 Cell proliferation

Proliferating cells manifest higher metabolic rate, increased nutrient uptake and morphological alterations, all of which are accompanied by volume changes. VRAC activity is cell cycle-dependent and correlates with cell proliferation. VRAC inhibition can induce cell cycle arrest in G0/G1 phase (Belsey et al. 2007), and vice versa, VRAC activity is significantly lower in this phase of cell cycle. In contrast, when cell cycle continues through the S phase, VRAC activity is increased; VRACs therefore probably play a role in G1/S checkpoint transition (Shen et al. 2000).

3.5.4 Migration

Migrating cells, e.g. tumor cells, readily change their shape to be able to get through narrow extracellular spaces. As it was demonstrated in highly invasive glioma cells, the mechanism involves extrusion of previously actively accumulated Cl^- ions, which allows the cells to shrink (Habela et al. 2009). Glioma and neuroblastoma cells display constitutively active VRACs under isotonic conditions, and it is hypothesized, that increased basal Cl^- conductance is an adaptive mechanism of malignant cells, facilitating uncontrolled proliferation and invasive migration. VRAC participation is further corroborated by the findings, that VRAC inhibitors, namely tamoxifen and NPPB, block both VRAC currents and cell migration with similar dose-dependent manner (Ransom et al. 2001).

3.5.5 Communication between astrocytes and neurons

As mentioned in the first chapter, increased neuronal activity leads to a rise in extracellular concentration of ions (mainly K^+) and neurotransmitters which must be removed in order to preserve proper neuronal functions. Maintenance of the homeostasis of neuronal environment is one of the key roles of perisynaptic astrocytes. They take up superfluous ions and neurotransmitters together with osmotically driven water. This results in astrocytic swelling and possibly activation of VRACs, which could constitute another pathway for astrocytic glutamate release and communication between astrocytes and neurons. In addition, extracellular ATP, released frequently by neurons as a co-transmitter, greatly enhances VRAC activity (Mongin et al. 2005). Tripartite synapse and neuronal activity-elicited astrocytic swelling and its consequences are schematically depicted in Figure 7. Astrocytes have also been shown to participate in the whole-body osmoregulation. Neurons in the supraoptic nucleus (SON) of hypothalamus are responsible for secretion of vasopressin, which regulates, among other bodily functions, water homeostasis. Astrocytes in the isolated SON release taurine in reaction to decreased extracellular osmolarity. Taurine than can act on neuronal glycine receptors and modulate vasopressin secretion and thus whole-body water homeostasis. Taurine efflux is inhibited by VRAC blockers (Deleuze et al. 1998).

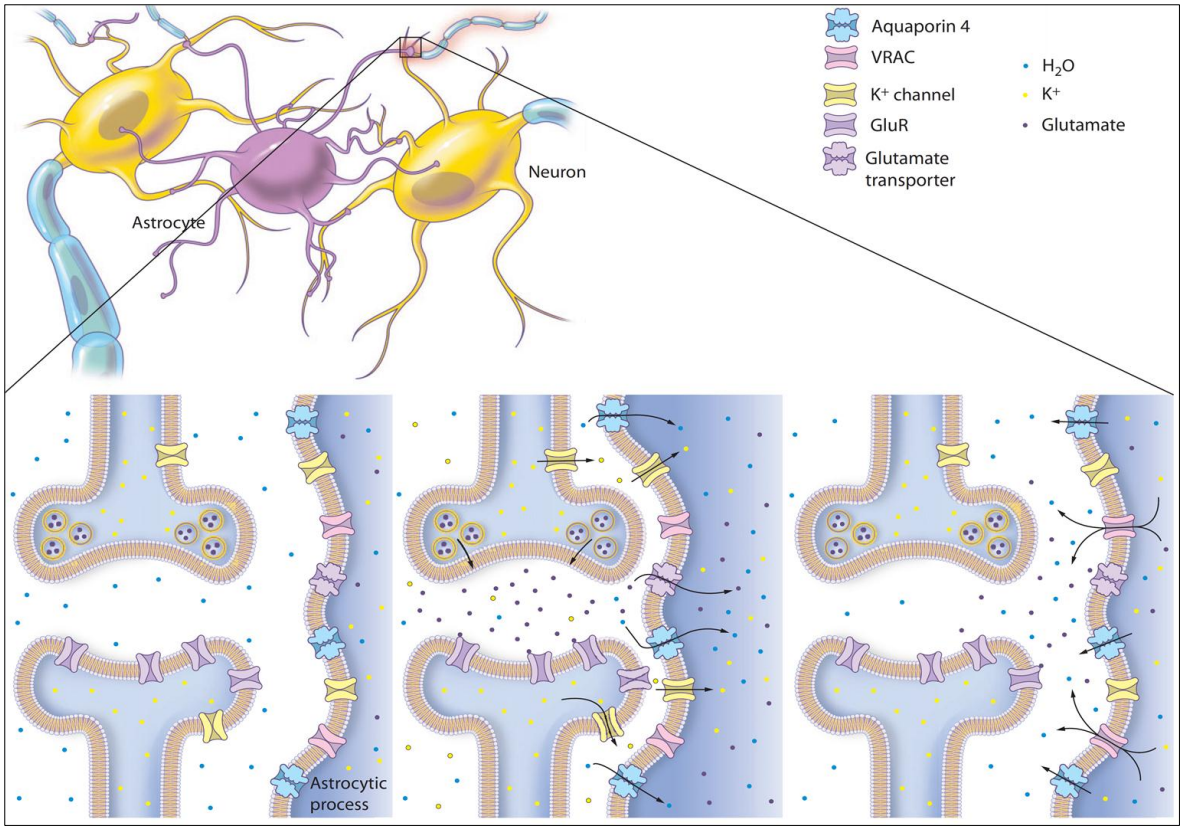

Figure 7. Schematic depiction of tripartite synapse and astrocytic swelling in response to neuronal activity. (Left) Inactive glutamatergic synapse. (Middle) Synaptic activity results in rise in extracellular K^+ and glutamate, which are subsequently taken up by astrocytes via respective channels and transporters, together with osmotically driven water, mainly through aquaporins. As a consequence, astrocytes swell and extrasynaptic space is reduced. (Right) VRACs open in reaction to swelling, allowing glutamate and Cl^- (not shown) to leave the cell, accompanied by water efflux via aquaporins, which results in cell volume recovery (Mulligan et al. 2006).

3.5.6 Brain swelling

Cellular swelling can be particularly detrimental in brain. The brain is encased by a rigid skull limiting the tissue expansion. Volume increase can thus lead to blood vessel constriction, brain parenchyma displacement and herniation and compression of autonomic centers in brain stem. On cellular level, cell swelling decreases extracellular space, which can cause neuronal hyperexcitability and neurotransmission failure, due to altered diffusion of signaling molecules and disrupted ionic homeostasis (Pasantes-Morales et al. 2002). Brain edema commonly occurs in various pathological states, such as ischemia, traumatic brain injury, acute liver failure or hyponatremia (Massieu et al. 2004; Kimelberg 2005). It is argued that neurons *in situ* and *in vivo* maintain their volume when exposed to hyposmotic environment because they lack functional aquaporins (Andrew et al. 2007; Risher et al. 2009). Astrocytes, on the other hand, readily swell in hyposmotic conditions. They express high levels of AQP4, localized predominantly at their perivascular endfeet, which makes their membrane easily permeable to water from bloodstream (Nase et al. 2008). Brain cells *in vivo* can encounter hyposmolarity during hyponatremia, elicited by inappropriate secretion of antidiuretic hormone, deficiency of adrenocortical hormones, hypothyroidism, some diuretics or renal or liver failure. Hyponatremia may cause brain edema and increased intracranial pressure (Pasantes-Morales et al. 2002). Animal models of chronic hyponatremia suggest that brain cells are able to continuously regulate their volume over a period of several days by RVD-like mechanism, indicated by decreased levels of inorganic and organic osmolytes, sustained for the duration of hyponatremic conditions (Massieu et al. 2004); however, no RVD could be directly observed in astrocytes *in situ* and *in vivo* (Hirrlinger et al. 2008; Risher et al. 2009).

Another common cause of astrocytic swelling is cerebral ischemia. Cerebral blood flow is transiently or permanently reduced during ischemia, compromising oxygen and

glucose supply to cells. In focal ischemia, or stroke, we can distinguish two regions – ischemic core and ischemic penumbra. The core receives no blood flow, whereas in the penumbra the blood flow is preserved to some extent. Tissue in the ischemic core is normally damaged beyond repair; however, cells in the penumbra remain more or less viable. Of all the brain cell types, neurons are especially prone to ischemic damage. Due to energy depletion, which is a consequence of oxygen end glucose deprivation, neuronal extracellular homeostasis is deteriorated during ischemia – the transmembrane ionic gradients are disrupted and there is a significant rise in extracellular K^+ and neurotransmitters, most importantly excitatory amino acid glutamate (Phillis et al. 2003; Mongin 2007). This glutamate overactivates neuronal glutamatergic receptors, causing uncontrolled rise in intracellular Ca^{2+}, activation of proteolytic cascades and eventually cell death. The main cause of astrocytic swelling during stroke is an increase in extracellular K^+ and accumulation of Na^+ and Cl^- resulting from the dysfunction of Na^+/K^+-ATPase due to energy depletion and altered ionic gradients. Swelling-induced activation of astrocytic VRACs, while beneficial for astrocytes because it helps them reduce their volume, further exacerbates excitotoxic neuronal damage, because it allows the flux of glutamate and aspartate from astrocytes into the extracellular space. Given that VRACs depend on intracellular ATP, VRAC-mediated excitotoxicity is more likely to occur in the ischemic penumbra than in the core, where ATP is rapidly depleted. In animal model of reversible middle cerebral artery occlusion (rMCAO), VRACs were shown to mediate substantial portion of excitatory neurotransmitters release (Feustel et al. 2004) and their inhibition with DCPIB attenuates glutamate release and reduces infarct size (Zhang et al. 2008).

AIMS OF THE THESIS

I. To characterize volume-regulated anion channels in primary culture of rat cortical astrocytes.

II. To clarify the impact of increased intracellular Na^+ concentration on volume-regulated anion channel activity in cultured cortical astrocytes

III. To explore astrocytic volume-regulated anion channels in the hippocampal CA1 region *in situ*

METHODS

1. PREPARATION OF ACUTE BRAIN SLICES

Ten to twelve-day-old rats (P10-12) were anesthetized with isoflurane (Abbott Laboratories, Chicago, IL, USA) and decapitated with iris scissors. Severed head was placed on a silicon coated Petri dish filled with cold (4°C) isolation solution, whose composition is listed in Table 1. The scalp was cut with microdissection scissors to expose the skull. After cutting the skull along the midline the skull bones were removed using dissecting tweezers. The olfactory bulb and cerebellum were cut off with scalpel and the rest of the brain was removed from the braincase and glued to the specimen disc with its ventral part leaning at a solid agar cube. The specimen disc was then placed in the buffer tray of the vibration microtome (Microm HM 650V, Thermo Fisher Scientific, Waldorf, Germany) containing cold isolation solution and 300 μm thick transverse slices were cut with razor blade. Slices were incubated in isolation solution warmed to 34°C in water bath for 30 minutes and subsequently held in artificial cerebrospinal fluid (aCSF, for composition see Table 1) at room temperature for the duration of the experiment (up to six hours).

Table 1. Extracellular solutions used for electrophysiological experiments in acute brain slices

Solution		Isolation solution	aCSF	Isotonic	Hypotonic
NaCl	[mM]		90	90	90
KCl	[mM]	3	3	3	3
NMDG-Cl	[mM]	110			
$NaHCO_3$	[mM]	23	28	28	28
Na_2HPO_4	[mM]	1.25	1.25	1.25	1.25
Glucose	[mM]	20	10	10	10
CsCl	[mM]			1	1
4-AP	[mM]			1	1
$BaCl_2$	[mM]			3	3
$CaCl_2$	[mM]	0.5	1.5	1.5	1.5
$MgCl_2$	[mM]	7	1.3	1.3	1.3
MFA	[mM]		0.1	0.1	0.1
pH		7.4	7.4	7.4	7.4
Osmolality [$mOsm \cdot kg^{-1}$]		300 ± 10	300 ± 10	300 ± 10	250 ± 10

2. PRIMARY ASTROCYTE CULTURES

Primary astrocyte cultures were prepared from male and female neonatal rat pups (P0 – P1). Rats were anesthetized with isofluran and decapitated in ice-cold ethanol. Scalp, skull bones and meninges were removed and the cortex was transferred into a sterile Petri dish using tweezers. Cortical tissue was mechanically dissociated in growth medium and the resulting suspension was filtered using sterile 70 μm cell strainer and poured into a culture flask. The final volume of the medium was brought to 5 – 6 ml. The cells were cultured in Dulbecco's modified Eagle's medium (DMEM, Gibco, Invitrogen, NY, USA) supplemented with penicillin/streptomycin (100 U/ml and 100 μg/ml, respectively, Gibco, Invitrogen, NY, USA) and 15% of heat inactivated fetal bovine serum (FBS, Gibco, Invitrogen, NY, USA) for the first week and 10% of heat inactivated FBS for the rest of cultivation period at 37°C in a 5% CO_2 humidified incubator. After reaching confluence, astrocytes were trypsinized and plated onto coverslips in 24-well culture plate at a concentration of 20000 cells/ml. Electrophysiological experiments were carried out 3–5 days later.

3. ELECTROPHYSIOLOGICAL EXPERIMENTS

Membrane currents were measured using patch-clamp technique in whole-cell configuration (Hamill, Marty et al. 1981). Micropipettes were pulled from borosilicate capillaries with filament (Sutter Instruments Company, Novato, CA, USA) using horizontal P-97 Flaming/Brown Micropipette Puller (Sutter Instruments Company, Novato, CA, USA) and had a resistance of 8 – 15 MΩ when filled with intracellular solution containing fluorescent dye (Alexa Fluor 594 hydrazide, 0.1 mM, Molecular Probes, Invitrogen, NY, USA) or Lucifer Yellow CH dilithium salt (Sigma-Aldrich, St. Louis, MO, USA) to facilitate post-recording cell identification. Specimens were transferred to a recording chamber mounted on the stage of an upright microscope (Axioskop 2, FS plus, Carl Zeiss, Oberkochen, Germany) equipped with a high-resolution digital camera (AxioCam HRc, Carl Zeiss, Oberkochen, Germany) and electronic micromanipulators (Luigs & Neumann, Ratingen, Germany). current signals were amplified by means of EPC-10 amplifier (HEKA Elektronik, Lambrecht, Germany) and lowpass-filtered at 3 kHz. Data acquisition, storage and analysis were performed with PatchMaster/FitMaster software (HEKA Elektronik, Lambrecht, Germany). Current patterns were obtained in the voltage-clamp mode and the resting

membrane potential (V_m) was measured by switching the amplifier to the current-clamp mode. The membrane resistance (R_I) was calculated from the current elicited by a 10-mV test pulse depolarizing the cell membrane from the holding potential of -70 mV to -60 mV for 50 ms. The steady-state current value was taken 40 ms after the onset of the depolarizing pulse. Membrane capacitance (C_m) was determined automatically from the LockIn protocol by Patch Master. Current densities (CDs) were calculated by dividing the maximum current amplitudes by the corresponding C_m for each individual cell. Osmolalities of all solutions were checked with a vapor-pressure osmometer (Vapro 5520, Wescor, South Logan, UT, USA), and when needed, adjusted with mannitol. pH values were estimated using pH-meter MiniLab IQ125 (IQ Scientific Instruments, Carlsbad, CA, USA).

Recording in primary astrocytic culture. Coverslips with astrocytic culture were placed in the recording chamber filled with standard solution. The standard solution was replaced with isotonic bath solution in order to block potassium conductance. Hypotonic solution was obtained by omitting mannitol from the isotonic solution. Compositions of extracellular solutions are given in Table 2. Continuous flux of solutions was achieved by means of gravity-driven perfusion system and peristaltic pump ensuring the outflow of solutions from the recording chamber. Two types of patch pipette solutions were used – intracellular CsCl solution and high-Na^+ solution, for composition see Table 3. To measure swelling-activated currents, cell membrane potential was held at 0 mV and voltage ramps of 1100 ms-duration ranging from -120 mV to 80 mV were applied.

Table 2. Extracellular solutions used for electrophysiological experiments in primary astrocyte culture

Solution	Standard	Isotonic	Hypotonic
NaCl [mM]	140		
KCl [mM]	4		
CsCl [mM]		122	122
HEPES [mM]	10	10	10
Glucose [mM]	5	5	5
$CaCl_2$ [mM]	2	2	2
$MgCl_2$ [mM]	2	2	2
pH, adjusted with	7.4, NaOH	7.4, CsOH	7.4, CsOH
Osmolality [mOsm·kg^{-1}]	300 ± 10	300 ± 10	250 ± 10

Table 3. Intracellular solutions used for recording in acute brain slices and primary astrocyte cultures

	Intracellular solutions for acute brain slices		Intracellular solutions for primary astrocyte culture	
Solution	KCl	CsCl	High – Na^+	CsCl
CsCl [mM]		140	90	140
KCl [mM]	130			
NaCl [mM]			50	
EGTA [mM]	5	1	1	1
HEPES[mM]	10	10	10	10
$CaCl_2$ [mM]	0.5			
MgATP[mM]	3	3		
$MgCl_2$ [mM]			2	2
pH	7.2	7.2	7.2	7.2
Osmolality [mOsm·kg^{-1}]	285 ± 5	285 ± 5	285 ± 5	285 ± 5

Recording in brain slices. Acute brain slices were held down in the recording chamber with a U-shaped platinum wire with a grid of nylon threads. The recording chamber was continuously perfused with recording solutions by means of peristaltic pump PCD 31.2 (Peristaltická čerpadla a dávkovače Ing. Jindřich Kouřil, Kyjov, Czech Republic) at a velocity of 5 ml/min. Bath solutions used were aCSF containing 100 µM meclofenamic acid (a gap-junction blocker, MFA; Sigma-Aldrich, St. Louis, MO, USA) and isotonic and hypotonic solution supplemented with potassium channel blockers. Their compositions are summarized in Table 1. The intracellular patch pipette solutions are listed in Table 3. For some experiments, 30 µM tamoxifen dissolved in dimethyl sulfoxide (both Sigma-Aldrich, St. Louis, MO, USA) or 20 µM DCPIB (Sigma-Aldrich, St. Louis, MO, USA) were added to the bath solution. All voltage protocols were delivered from a holding potential of -70 mV. Different components of the whole-cell currents were obtained by means of following protocols: inwardly rectifying potassium currents (K_{IR}) was acquired by clamping the cell from the holding potential of -70 mV to values ranging from -160 to 40 mV in 10-mV voltage increments (50 ms duration). K_{IR} amplitude was determined at -140 mV, 40 ms after the onset of hyperpolarizing pulse. In order to isolate delayed outwardly rectifying K^+ currents (K_{DR}), stepping of the cell membrane potential from -100 to 40 mV in 10-mV increments was preceded by a prepulse depolarizing the membrane to -50 mV for 100 ms to inactivate the

transient inactivating A-type potassium currents (K_A). K_{DR} currents amplitudes were subsequently measured at 40 mV, 40 ms after the onset of depolarizing pulse, , after subtracting offline the time- and voltage-independent passive currents between -70 mV and -60 mV multiplied by the relative potential jumps. Maximal activation of the K_A currents was achieved by a -110-mV prepulse and its amplitude, measured at 40 mV at the beginning of the pulse when the currents reached its peak value, was obtained by subtracting the currents traces pre-clamped at -50 mV from those pre-clamped at -110 mV. The protocol used for measuring of the swelling-activated currents was a voltage ramp ranging from -100 mV to 100 mV.

4. IMMUNOCYTOCHEMISTRY AND IMMUNOHISTOCHEMISTRY

Cells attached to cover slips were fixed using 4% paraformaldehyde in 200 mM phosphate buffer (45.2 mM NaH_2PO_4, 154.8 mM Na_2HPO_4, pH 7.4; Sigma-Aldrich, St. Louis, MO, USA) for 15 min and rinsed twice with phosphate buffer saline (10 mM phosphate buffer, 150 mM NaCl, pH 7.4; Sigma). To permeabilize cell membranes and prevent non-specific staining, cells were incubated for 2 hours in blocking buffer (10 mM PBS containing 0.5% Triton; Sigma and 5% Chemiblocker; Millipore, Billerica, MA, USA). Subsequently, cells were incubated with primary antibody, mouse anti-GFAP (Cy3-conjugate; 1:800 Sigma-Aldrich, St. Louis, MO, USA) diluted in blocking buffer at 4ºC overnight. Superfluous antibodies were washed away with PBS. To visualize the cell nuclei, the coverslips were mounted using Vectashield mounting medium containing 4',6-diamidino-2-phenylindole (DAPI; Vector Laboratories, Burlingame, MI, USA).

Brain slices underwent 45 – 60 minute-long fixation with 4% PFA followed by rinsing (3 x 10 minutes) with cold PBS. The slices were incubated for 2 hours in blocking buffer, rinsed with PBS (3 x 10 minutes) and incubated with primary antibody, rabbit anti-NG2 (1:400, Millipore, Billerica, MA, USA) at 4ºC overnight. The secondary antibody, goat anti-rabbit IgG conjugated with Alexa Fluor 594 (1:200; Molecular Probes, Invitrogen, Grand Island, NY), was applied for 2 hours at room temperature. All antibodies were diluted in blocking buffer. After immunostaining, the slices were rinsed with PBS (3 x 10 minutes) and mounted on microscope slides using Vectashield mounting medium with DAPI (Vector Laboratories, Burlingame, MI, USA).

5. CONFOCAL MICROSCOPY

To carry out immunocyto/immunohistochemical analysis, a Zeiss 510DUO LSM equipped with Arg/HeNe lasers and 40x oil objective was employed. Stacks of consecutive confocal images taken at intervals of 1 μm were acquired sequentially with the 2 lasers to avoid cross-talk between fluorescent labels. The background noise of each confocal image was reduced by averaging four image inputs. For each image stack the gain and detector offset were adjusted to minimize saturated pixels, yet still permit the detection of weakly stained cell processes.

6. DATA ANALYSIS

Data are presented as means ± standard error of the mean. The statistical significance of the differences before and after treatment in the same experimental group was assessed by paired t-test using SigmaPlot software (Systat Software, San Jose, CA, USA). Differences were considered significant (*) at $p \in (0.01; 0.05)$,very significant (**) at $p \in (0.001; 0.01)$ and extremely significant (***) at $p < 0.001$. All graphs were created using SigmaPlot software.

RESULTS

1. VOLUME-REGULATED ANION CHANNELS IN RAT PRIMARY ASTROCYTE CULTURE

1.1 Morphological and electrophysiological properties of astrocytes in rat primary culture

We prepared primary astrocyte culture from cerebral cortices of neonatal rat pups (see Methods). The cells were used for experiments between 3 and 5 weeks of cultivation. Immunostaining for glial fibrillary acidic protein (GFAP) and the flat, polygonal morphological phenotype of the cultured cells indicated that under our cultivation conditions, more than 95% of cells were type-1 cortical astrocytes. To further characterize astrocytes in rat primary culture, we assessed their passive membrane properties (V_m, R_I and C_m) and current patterns using the patch-clamp method in the whole-cell configuration. The morphology and current patterns of cultured astrocytes are depicted in Figure 8 and their passive membrane properties are summarized in Table 4. All astrocytes displayed outwardly rerctifying current in response to hyper- and depolarizing pulses from -160 to 40 mV (Figure 8D).

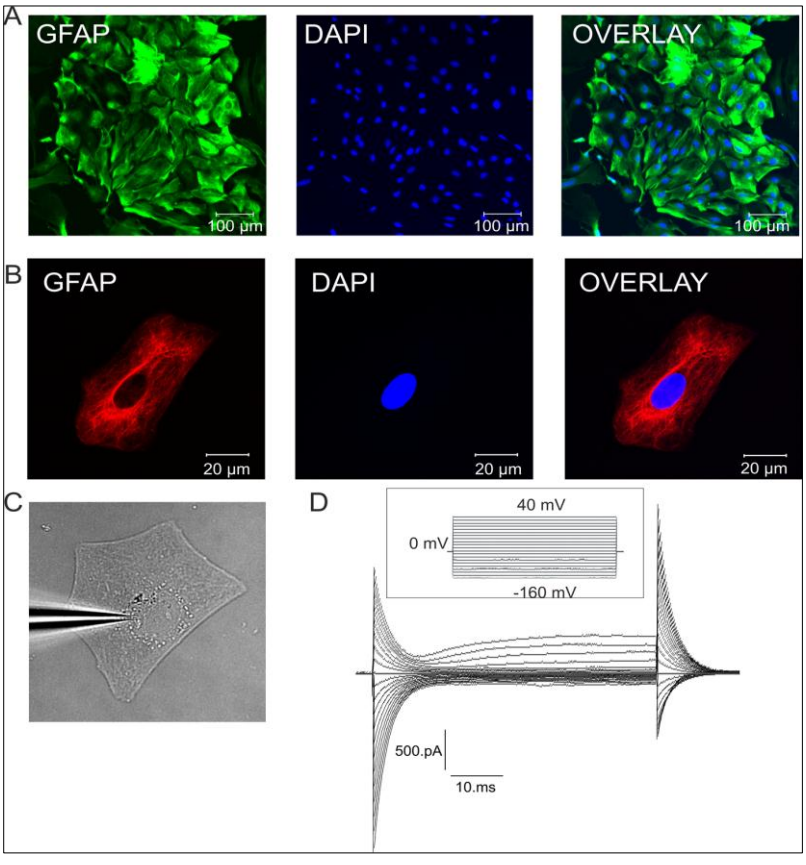

Figure 8. Morphology and current patterns of astrocytes in rat primary culture. **(A)** Immunostaining of rat primary astrocyte culture. Astrocytes were stained with mouse anti-GFAP antibody. Cell nuclei were visualized using 4',6-diamidino-2-phenylindole (DAPI). **(B)** Immunostainning of single astrocyte. **(C)** Photomicrograph of an astrocyte during recording. **(D)** Representative currents traces elicited by 50-ms-long voltage steps applied every 10 ms from -40 mV to potentials ranging from -160 to 40 mV (see inset).

Table 4. Passive membrane properties of astrocytes in rat primary culture

V_m [mV], n = 7	R_I [MO], n = 6	C_m [pF], n = 7
-27.71 ± 2.83	830.49 ± 239.14	44 ± 8.26

Values given are means ± standard error of the mean (SEM).

1.2 Hypotonic stress activates volume-regulated anion channels in rat primary astrocyte culture

Astrocytes exposed to hypotonic stress regulate their volume via controlled release of osmolytes. Volume-regulated anion channels serve as one of the pathways underlying osmolyte efflux. In order to activate VRACs, cells were exposed to hypotonic solution (250 mOsmol/kg). Current densities in isotonic solution were -3.78 ± 1.41 pA/pF at -120 mV and 11.38 ± 2.48 pA/pF at 80 mV. After switching to hypotonic solution, we recorded a significant increase in currents to -29.66 ± 6.23 pA/pF and 38.77 ± 7.42 pA/pF at -120 mV and 80 mV, respectively (n = 7). Representative traces of currents in isotonic and hypotonic solutions and current densities are depicted in Figure 9. In order to explore pharmacological properties of hypotonicity-induced conductance, we employed a selective VRAC blocker, 10 μM DCPIB. Under our experimental conditions, DCPIB inhibited hypotonicity-induced currents by ~ 75 % (n = 10, Figure 10).

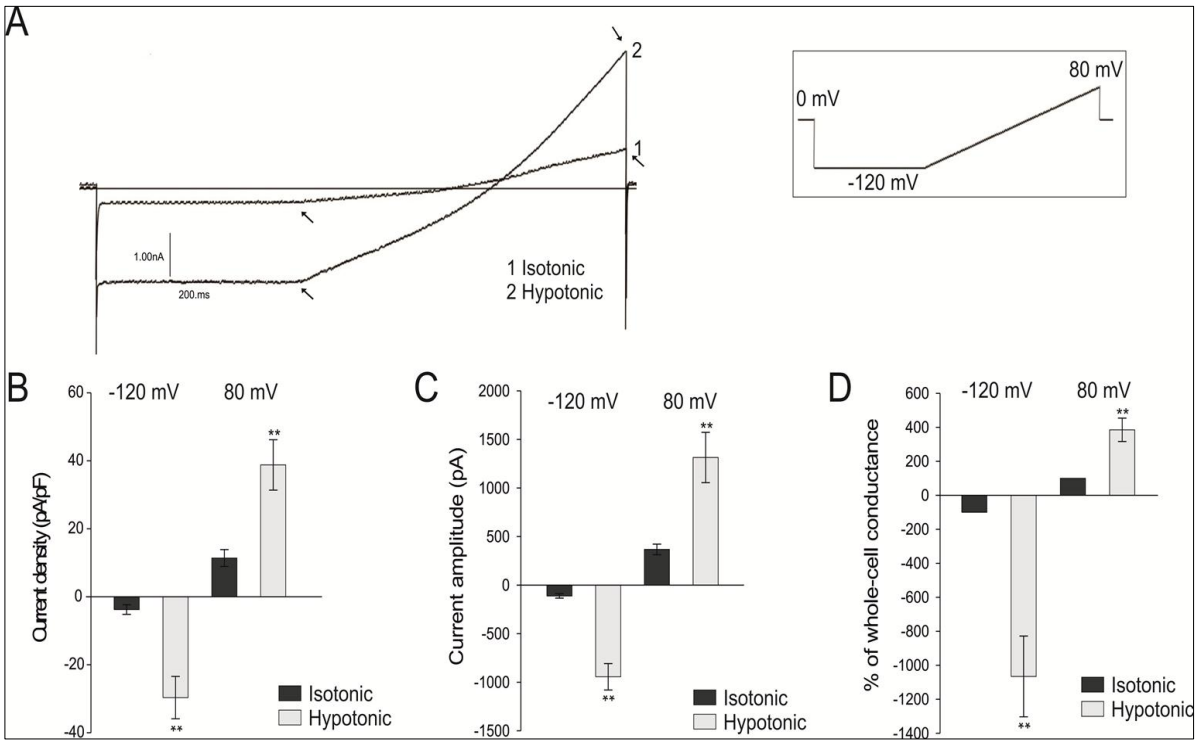

Figure 9. Hypotonicity-induced activation of VRAC currents in rat primary astrocyte culture (A) currents traces elicited by a ramp protocol obtained in isotonic (1) and hypotonic (2) solutions. Average currents densities **(B)**, currents amplitudes **(C)** and percentage change in whole cell conductance under isotonic conditions and hypotonic stress at -120 mV and 80 mV. Astrocytes (n = 7) were clamped at a holding potential of 0 mV and voltage ramps from -120 mV to 80 mV were applied. currents amplitudes were measured at voltages indicated by arrows. Statistical significance was calculated using paired t test. Data are given as a mean ± SEM, **p < 0.01.

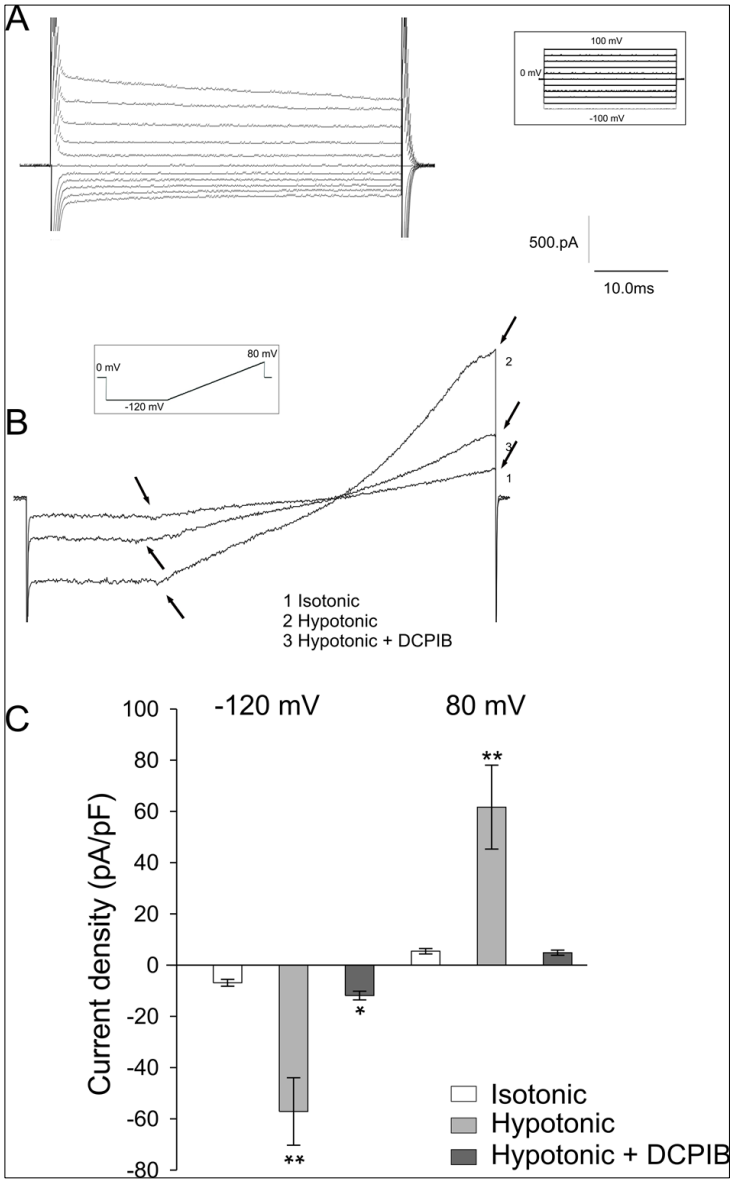

Figure 10. Electrophysiological and pharmacological characte-ristics of hypotonicity-induced currents in rat cultured cortical astrocytes

(A) Representative current traces recorded in hypotonic solution and elicited by stimulating the cells by voltage pulses ranging from -100 mV to 100 mV from a holding potential of 0 mV (see inset). Note the current deactivation at positive potentials. **(B)** Current traces elicited by a voltage ramp pulse (see inset) under (1) control conditions, (2) after application of hypotonic solution and (3) in the presence of DCPIB (n = 10). **(C)** Average densities of currents elicited under control conditions, upon hypotonic stres and in the presence of DCPIB. Statistical significance was calculated using paired *t* test. Data are given as a mean ± SEM, **p < 0.01 compared to control (isotonic solution).

1.3 Increased intracellular Na^+ inhibits hypotonicity-induced currents

Various CNS insults, such as ischemia/reperfusion, can lead to substantial increase in intracellular Na^+ concentration. During oxygen-glucose deprivation, a widely used *in vitro* model of ischemia (Benesova et al. 2009; Benesova et al. 2012), $[Na^+]_i$ can rise up to 50 mM (Lenart et al. 2004). Therefore, we next sought to elucidate the effect of 50 mM intracellular Na^+ concentration on VRAC activity.

For this purpose, we replaced control CsCl intracellular solution with 50 mM Na^+. We observed a strong inhibitory effect of increased intracellullar Na^+ on hypotonicity induced currents. Seven cells recorded with control CsCl-intracellular solution showed approximately 7.8-fold increase in currents density magnitude after switching to hypotonic solution at -100 mV and 3.4-fold increase at 100 mV, whereas currents density in cells patched with high-Na^+ intracellular solution (n = 10) increased only approximately 1.81-fold under hypotonic stress at -100 mV and 1.95-fold at 100 mV (Figure 11).

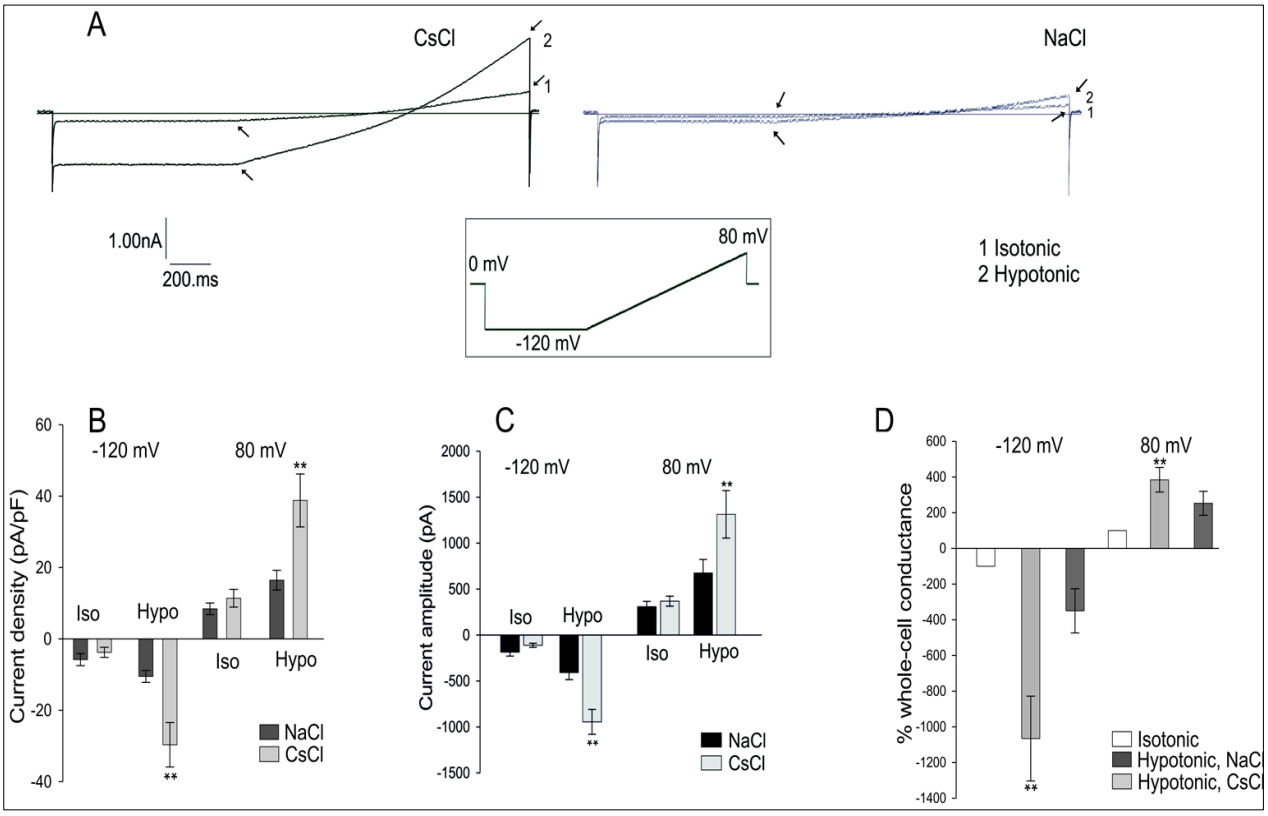

Figure 11. Increased intracellular Na^+ inhibits hypotonicity-induced VRAC current activation.

(A) Current traces elicited by a ramp protocol obtained in isotonic (1) and hypotonic (2) solutions. Average current densities **(B)**, current amplitudes **(C)** and percentage change in whole cell conductance under isotonic conditions and hypotonic stress at -120 mV and 80 mV. Astrocytes from primary cortical cultures were clamped at a holding potential of 0 mV and voltage ramps from -120 mV to 80 mV were applied. Current amplitudes were measured at voltages indicated by arrows. Statistical significance was calculated using paired *t* test. Data are given as a mean ± SEM, **p < 0.01 compared to control (isotonic solution).

2. VOLUME-REGULATED ANION CHANNELS IN ACUTE RAT BRAIN SLICES

2.1 Morphological and electrophysiological properties of astrocytes *in situ*

Acute brain slices from juvenile rats were prepared as described in Methods. For electrophysiological recordings, we have chosen cells from the stratum radiatum or stratum oriens of the hippocampus. Astrocytes were identified based on their morphology, electrophysiological properties (V_m, R_I, C_m and current patterns) and post-recording immunohistochemistry. Astrocytes *in situ* displayed typical morphology, characterized by numerous highly branched processes, and they expressed time- and voltage-independent, symmetrical non-decaying K^+ currents (passive current pattern) as described previously (Zhou et al. 2006). The morphology and current patterns of *in situ* astrocytes are depicted in Figure 12. Passive membrane properties are summarized in Table 5. Since GFAP level in astrocytes of young animals are quite low and therefore difficult to detect, we relied mostly on morphological and electrophysiological features of cells to identify astrocytes suitable for recording. However, to exclude the possibility of having mistakenly recorded NG2-glial cells that might express similar properties as immature astrocytes (Butt et al. 2002), we have used antibody against NG2 chondroitin sulphate proteoglycan (NG2). Therefore, NG2-negative cells displaying passive membrane current pattern were considered astrocytes.

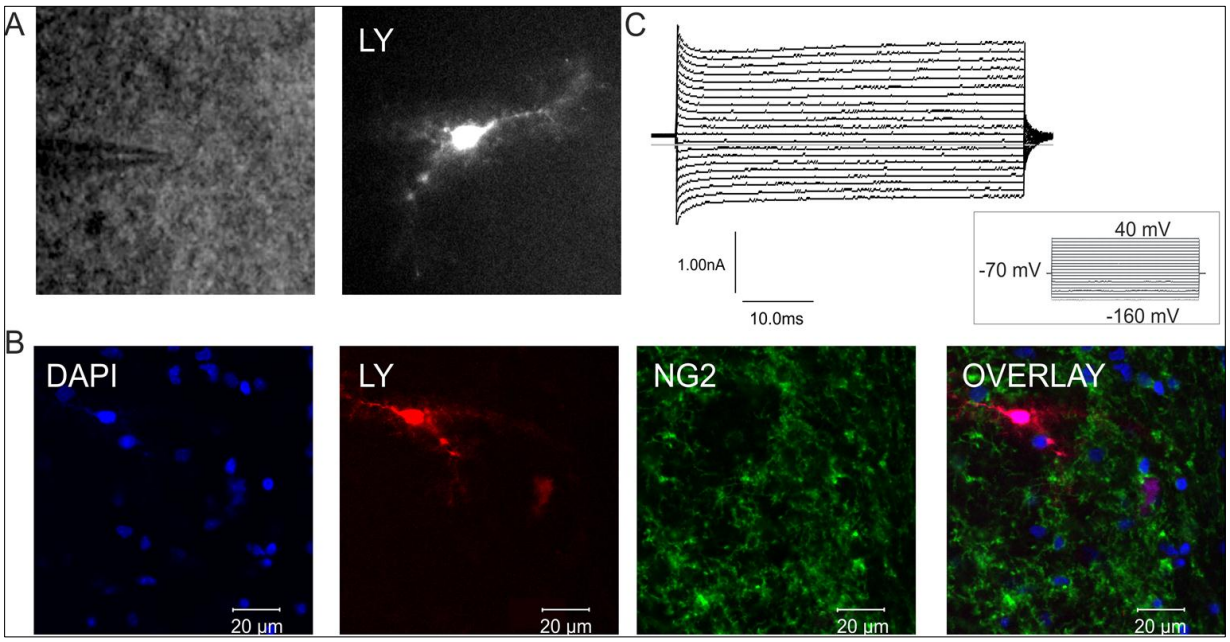

Figure 12. Morphological and electrophysiological properties of astrocytes in acute rat brain slices.

(A) Photomicrograph of and fluorescent micrograph a hippocampal astrocyte filled with Lucifer yellow during patch-clamp recording. **(B)** Post-recording immunohistochemical identification of the recorded astrocyte. The cell was stained with rabbit anti-NG2 antibody. Cell nuclei were visualized using 4',6-diamidino-2-phenylindole (DAPI). **(C)** Representative current traces elicited by 50-ms-long voltage steps applied every 10 ms from -40 mV to potentials ranging from -160 to 40 mV (see inset).

Table 5. Passive membrane properties of astocytes in acute rat brain slices

V_m [mV]	-81 ± 1.28	n = 17
R_I [MO]	85.59 ± 8.07	n = 17
C_m [pF]	39.33 ± 2.29	n = 34

Values given are means ± standard error of the mean (SEM).

2.2 Identification of VRACs *in situ*

In order to record membrane currents from individual astrocytes in stratum radiatum or stratum oriens of hippocampus in acute brain slices, interastrocytic gap junction coupling was inhibited. For this purpose, we added 100 µM meclofenamic acid (MFA), a gap junction blocker (Schools et al. 2006), to all extracellular solutions. To isolate volume-regulated anion

currents, we inhibited the dominant K^+ conductance by using CsCl-based pipette solution and adding K^+ channel blockers to isotonic and hypotonic external solutions (see Methods). Under these conditions, we were able to inhibit resting whole-cell membrane conductance by 72.66 ± 3.39 % as depicted in Figure 13 (n = 17).

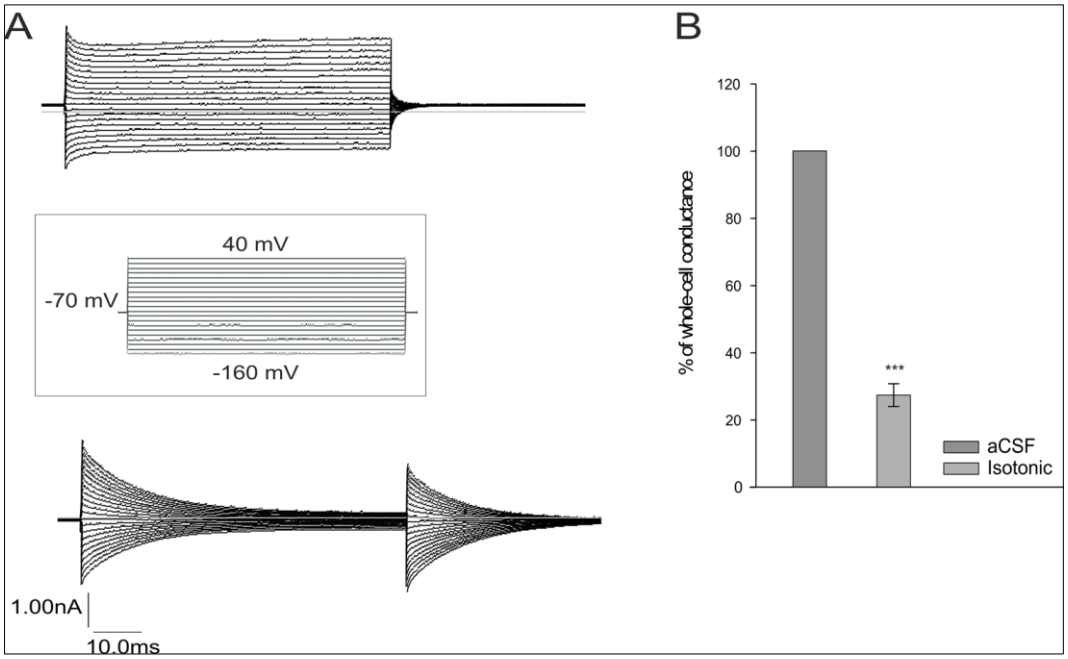

Figure 13. Inhibition of whole-cell gap junction and potassium conductance. Representative traces of whole-cell membrane currents under **(A)** control condition and **(B)** after application of 100 µM MFA,1 mM 4-AP, 1 mM CsCl and 3 mM $BaCl_2$. *In situ* hippocampal astrocytes were clamped at a holding potential of -70 mV and 50-ms voltage steps from -160 to 40 mV in 10-mV increments were applied. **(C)** The percentage change in whole-cell conductance after addition of the inhibitors. Statistical significance was calculated using paired *t* test, *** $p < 0.001$.

2.3 VRAC activation *in situ*

In order to elicit cell swelling and consequently the activation of volume-regulated anion channels, hypotonic solution (250 mOsmol/kg) was applied. Current densities recorded in isotonic solution were 1.63 ± 0.18 pA/pF at -100 mV and 6.96 ± 0.90 at 100 mV. After switching to hypotonic solution, in 4 cells out of 11, we observed an increase in current densities to 2.19 ± 0.32 pA/pF at -100 mV and to 7.58 ± 1.10 pA/pF at 100 mV (n = 4; Figure 14).

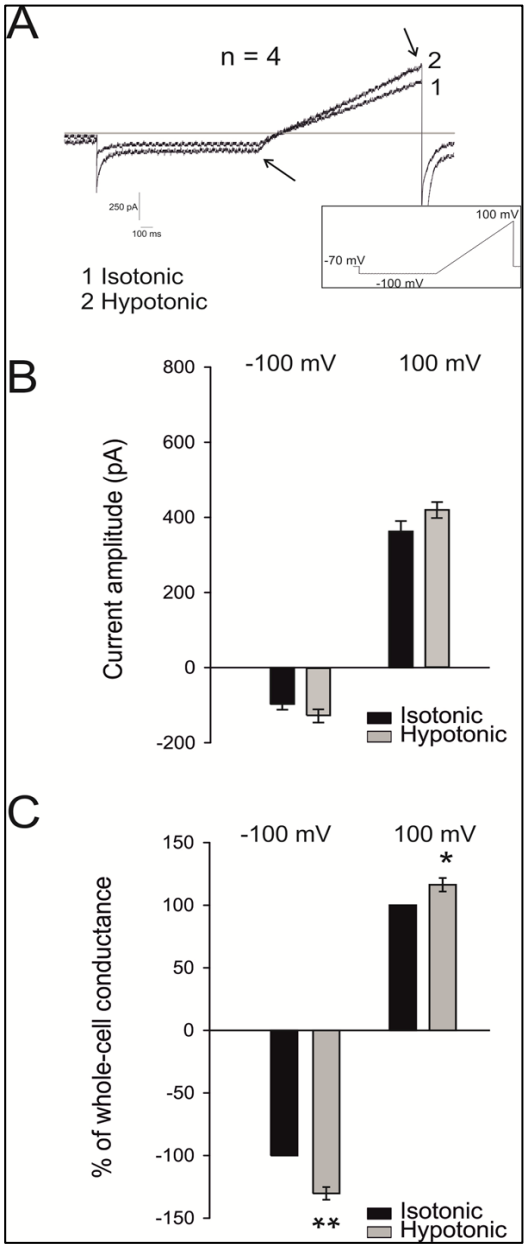

Figure 14. Hypotonicity-induced VRAC activation *in situ*

(A) Representative current traces of astrocytic response to hypotonic stress **(B)** average values of current amplitudes in isotonic and hypotonic solutions **(C)** percentage change in whole-cell conductance in response to hypotonic stress at -100 mV and 100 mV. *In situ* hippocampal astrocytes were clamped at a holding potential of -70 mV and voltage ramps from -100 mV to 100 mV were applied (see inset). Data represent mean values ± SEM, *p < 0.05, **p < 0.01 compared to control.

2.4 Pharmacological properties of VRACs in situ

To investigate pharmacological properties of VRACs in astrocytes *in situ*, we added two widely used VRAC inhibiting agents – 30 µM tamoxifen (Tx, n = 20) or 20 µM DCPIB (n = 5), the most selective VRAC blocker reported to date, into the hypotonic solution. Both inhibitors prevented the activation of VRAC currents induced by hypotonic stress. While hypotonic solution alone increased the inward and outward currents by ~ 30% and 16%, respectively, in the presence of DCPIB or tamoxifen, the increase in conductance was not

observed (Fig. 15).

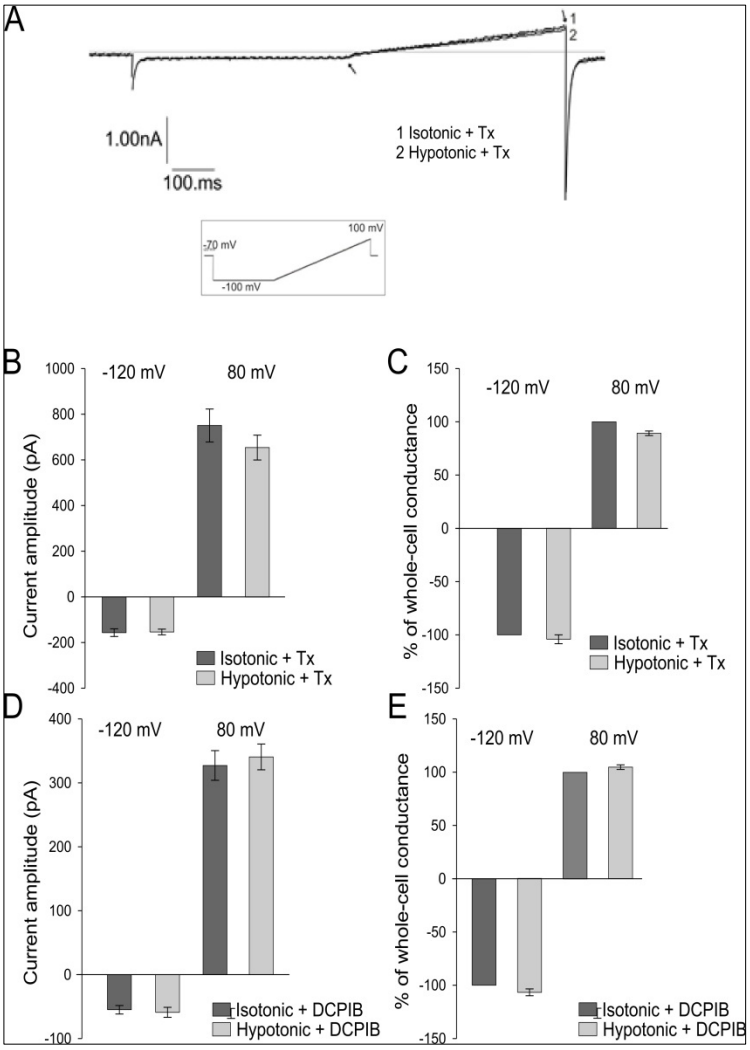

Figure 15. Pharmacological properties of hypotonicity-induced activation of VRAC currents.
(A) Representative current traces, **(B)** Current amplitudes and **(C)** percentage change in the whole-cell conductance under isotonic recorded after addition of 30 µM tamoxifen (Tx) (n = 20) to external recording solutions. Tamoxifen prevented the hypotonicity-induced activation of VRAC currents. **(D)** Current amplitudes and **(E)** percentage change in the whole-cell conductance after application of 20 µM DCPIB (n = 5). DCPIB also prevented hypotonicity-induced VRAC activation. Data represent mean values ± SEM, **p < 0.01.

DISCUSSION

We have performed a comprehensive analysis of volume-regulated anion channels in rat astrocytes demonstrating VRAC activity induced by hypotonic stress in both cultured cortical astrocytes as well as hippocampal astrocytes *in situ*. Additionally, we have shown that activity of VRACs is strongly dependent on intracellular Na^+ levels.

VRACs in rat primary astrocyte cultures

We prepared rat primary astrocyte cultures, whose morphological and biochemical properties were comparable to those of type 1 cortical astrocytes described elsewhere (Ferroni et al. 1995) – the cells had flat, polygonal shape and stained positively for GFAP. Compared to astrocytes *in situ*, cultured astrocytes had more positive V_m and higher R_I, whereas their C_m was not significantly different. Cultured astrocytes differ from astrocytes *in situ* also with respect to electrophysiological phenotypes – while astrocytes *in situ* are electrophysiologicaly passive, cultured astrocytes are rather outwardly rectifying and expressed minimal inward currents, which are features reminiscent of immature astrocytes (Zhou et al. 2006). More positive V_m and high R_I in cultured astrocytes possibly originate from the lack of two-pore domain K^+ channels and K_{IR} channels, which have been shown *in situ* to maintain negative V_m (Djukic et al. 2007; Seifert et al. 2009) and also contribute to high passive K^+ conductance (Zhou et al. 2009). In agreement with previous studies, we found that cultured astrocytes, significantly increase their whole-cell membrane conductance when exposed to hypotonic challenge (Pasantes-Morales et al. 1994, Crepel et al. 1998, Abdullaev et al. 2006). Electrophysiological characteristics of the observed currents, such as mild outward rectification and time-dependent inactivation at positive potentials are in agreement with those described for VRACs (Okada 1997). Of note, 10 μM DCPIB blocked ~75% of hypotonicity-evoked current, while Benfenati and co-authors (2009) observed complete inhibition of this current in cultured cortical astrocytes. Such a discrepancy can be explained by the fact, that we use Wistar rats, whereas Benfenati and co-authors use Sprague-Dawley rats.

Interestingly, we found that VRAC activity is strongly dependent on $[Na^+]_i$. Intracellular Na^+ influences various membrane transport processes, such as K^+ and glutamate uptake (Kahle et al. 2009) and it markedly alters during physiological as well as pathological processes, such as metabolic Na^+ waves and ischaemic stroke, respectively. Indeed, during

these events, $[Na^+]_i$ can reach up to 25-60 mM (Rose et al. 1998, Lenart et al. 2004). During pathological states, increase in $[Na^+]_i$ can result in reversal of Na^+-dependent glutamate transporters (Phillis et al. 2000) and Na^+/Ca^{2+} exchanger (NCX, Dietz et al. 2007), which leads to cellular swelling, accumulation of extracelluar glutamate and consequently, to excitotoxic neuronal death. Another result of NCX reversal is an increase in $[Ca^{2+}]_i$, eventually resulting in programmed cell death of astrocytes, which occurs at late stages following ischemia (Anderova et al. 2011). Our unpublished data (Figure 16) revealed that even small increases in $[Na^+]_i$ decrease VRAC activity and at 50 mM $[Na^+]_i$ VRACs are almost completely abolished. This suggests that astrocytes exposed to severe ischemia might lose their ability to regulate their volume, ultimately leading to astrocytic damage. On the other hand, such inhibition of VRACs by increased intracellular $[Na^+]_i$ could represent an endogenous neuroprotective mechanism as astrocytic VRACs are thought to exacerbate excitotoxic neuronal damage by allowing the efflux of excitatory amino acids under pathological conditions associated with astrocytic swelling (Kimelberg et al. 1990, Feustel et al. 2004). In contrast to our findings, increased $[Na^+]_i$ concentration was shown to activate VRACs in hippocampal neurons in situ (Zhang et al. 2011). Nonetheless, different experimental approaches, such as cell type, cell culture versus tissue slices or different pathological stimuli could cause this discrepancy.

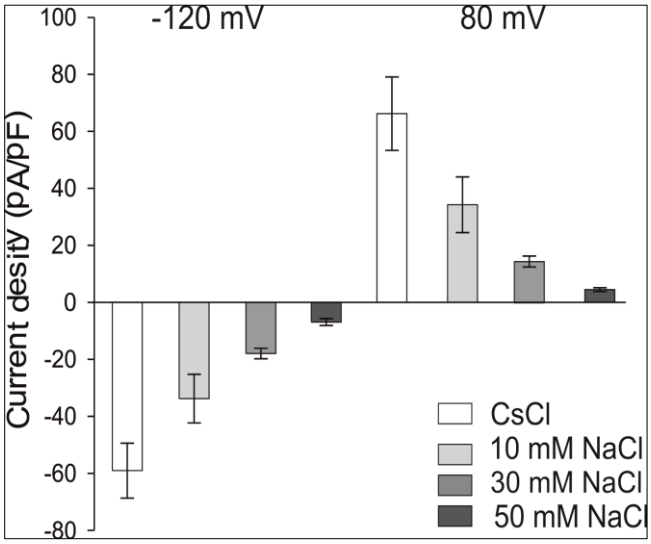

Figure 16. The impact of increasing intracellular Na^+ concentrations on hypotonicity induced VRAC activity in cultured astrocytes.
Graph summarizing the effect of intracellular Na^+ on VRAC activity. Note that 50 mM Na^+ reduced VRAC activity by ~ 88%.

VRACs in *in situ* astrocytes

VRACs were comprehensively studied and described in cultured cells; however, data from *in situ or in vivo* experiments are scarce. More importantly, VRAC activity *in situ*/*in*

vivo has been mainly assessed indirectly, based on the amount of excitatory amino acids released into the extracellular space (Feustel et al. 2004; Estevez et al. 1999; Zhang et al. 2008). Therefore, while interpreting such results, one must take into consideration other mechanisms mediating amino acid efflux, such as Ca^{2+}-dependent exocytosis, reversal of amino acids transporters (Feustel et al. 2004), connexin hemichannels (Ye et al. 2009) or maxi-anion channels (Liu et al. 2006).

Using patch-clamp technique Inoue and co-authors (2007) described swelling-activated channels with typical VRAC properties (outward rectification, dependence on intracellular ATP, inactivation at positive potentials) in cortical neurons in mouse brain slices. Another group observed hypotonicity-activated VRAC-like currents in CA1 neurons in rat hippocampal slices; however these currents were not sensitive to VRAC blockers, such as tamoxifen or DCPIB, suggesting that they may be mediated by other anion channels (Zhang et al. 2011).

In our experiments, we focused on rat hippocampal astrocytes. Upon exposure to hypotonic solution, astrocytes increased their whole-cell conductance, which is in good agreement with findings *in vitro* (Okada 1997, Parkerson et al. 2004, Abdullaev et al. 2006) as well as in neurons *in situ* (Inoue et al. 2005; Zhang et al. 2011). Surprisingly, under our experimental conditions, we have detected VRAC-like current only in less than 50% of recorded astrocytes and furthermore, compared to *in vitro* experiments, hypotonicity-induced currents were rather small. However, since it has been shown that carbenoxolone, a gap junction blocker, reduces VRAC mediated glutamate and taurine release in cultured rat cortical astrocytes (Benfenati et al., 2009), we suggest that VRAC current amplitudes, as well as VRAC incidence, might be affected by employing MFA to block astrocytic gap junctions. Moreover, recently published data showed that a substantial heterogeneity exists between astrocytes even within individual brain regions (Matyash et al. 2009), which might account for different behaviour of astrocytes exposed to hypotonic stress. Indeed, Chvatal et co-authors (2007) described two astrocytic subpopulations of cortical astrocytes *in situ* based on their distinct volume changes during hypotonic challenge. Although experiments employing *in vivo/in situ* astrocyte imaging did not confirm the existence of RVD in astrocytes (Hirrlinger et al. 2008, Risher et al. 2009), our preliminary data obtained by 3D-confocal morphometry revealed the existence of a subpopulation of cortical astrocytes effectively regulating cell volume during hypotonic stress (unpublished data).

As expected from our data obtained *in vitro* the DCPIB and tamoxifen prevented the activation of VRACs in response to hypotonic stress. Interestingly, after tamoxifen

application, we observed even a decrease in outward currents recorded under hypotonic conditions. Besides inhibiting VRACs, tamoxifen is known to influence various cellular processes, therefore such conductance inhibition might be also due to its other effects. For example, tamoxifen has been shown to affect plasmalemal voltage-dependent anion channels (pl-VDAC) via phosphatases activation and pl-VDAC dephosphorylation (Herrera et al. 2011) or blocks hemichannels (Ye et al. 2009).

The molecular identity of VRACs is still a matter of debate. Despite the fact that chloride channels ClC-2, 3, 4 and 5, VDACs and Ca^{2+}-sensitive Cl^- channels were excluded as VRACs candidates (Abdullaev et al., 2006), Benesova and co-authors (2012) showed the existence of astrocytic subpopulation expressing high levels of mRNA for ClC-2 and displaying effective cell volume regulation, which was partially abolished by DCPIB. This suggests that ClC-2 channels might, at least partially, contribute to hypotonicity-induced conductance.

CONCLUSIONS

In conclusion, we confirmed that rat cultured cortical astrocytes express VRACs and moreover, we demonstrated that VRACs are regulated by intracellular Na^+. Furthermore, we reported for the first time, that hippocampal astrocytes *in situ* possess VRACs, which makes them a prospective target for therapy of pathologies accompanied by cytotoxic brain edema, most importantly ischemia or traumatic brain injury.

REFERENCES

Abdullaev, I. F., et al. (2006). "Pharmacological comparison of swelling-activated excitatory amino acid release and Cl- currents in cultured rat astrocytes." J Physiol **572**(Pt 3): 677-689.

Abdullaev, I. F., et al. (2003). "Upregulation of swelling-activated Cl- channel sensitivity to cell volume by activation of EGF receptors in murine mammary cells." J Physiol **549**(Pt 3): 749-758.

Anderova, M., et al. (2011). "Cell death/proliferation and alterations in glial morphology contribute to changes in diffusivity in the rat hippocampus after hypoxia-ischemia." J Cereb Blood Flow Metab **31**(3): 894-907.

Andrew, R. D., et al. (2007). "Physiological evidence that pyramidal neurons lack functional water channels." Cereb Cortex **17**(4): 787-802.

Azevedo, F. A., et al. (2009). "Equal numbers of neuronal and nonneuronal cells make the human brain an isometrically scaled-up primate brain." J Comp Neurol **513**(5): 532-541.

Belsey, M. J., et al. (2007). "Inhibition of ERK and JNK decreases both osmosensitive taurine release and cell proliferation in glioma cells." Neurochem Res **32**(11): 1940-1949.

Benesova, J., M. Hock, O. Butenko, I. Prajerova, M. Anderova and A. Chvatal (2009). "Quantification of astrocyte volume changes during ischemia in situ reveals two populations of astrocytes in the cortex of GFAP/EGFP mice." J Neurosci Res 87(1): 96-111.

Benesova, J., et al. (2012). "Distinct expression/function of potassium and chloride channels contributes to the diverse volume regulation in cortical astrocytes of GFAP/EGFP mice." PLoS One **7**(1): e29725.

Benfenati, V., et al. (2007). "Expression and functional characterization of transient receptor potential vanilloid-related channel 4 (TRPV4) in rat cortical astrocytes." Neuroscience **148**(4): 876-892.

Benfenati, V. and S. Ferroni (2009). "Water transport between CNS compartments: functional and molecular interactions between aquaporins and ion channels." Neuroscience.

Benfenati, V., et al. (2007). "Functional down-regulation of volume-regulated anion channels in AQP4 knockdown cultured rat cortical astrocytes." J Neurochem **100**(1): 87-104.

Bernardinelli, Y., et al. (2004). "Astrocytes generate Na+-mediated metabolic waves." Proc Natl Acad Sci U S A **101**(41): 14937-14942.

Bonansco, C., et al. (2011). "Glutamate released spontaneously from astrocytes sets the threshold for synaptic plasticity." Eur J Neurosci **33**(8): 1483-1492.

Bushong, E. A., et al. (2002). "Protoplasmic astrocytes in CA1 stratum radiatum occupy separate anatomical domains." J Neurosci **22**(1): 183-192.

Butt, A. M., J. Kiff, P. Hubbard and M. Berry (2002). "Synantocytes: new functions for novel NG2 expressing glia." J Neurocytol 31(6-7): 551-565.

Butt, A. M. and A. Kalsi (2006). "Inwardly rectifying potassium channels (Kir) in central nervous system glia: a special role for Kir4.1 in glial functions." J Cell Mol Med **10**(1): 33-44.

Cahoy, J. D., et al. (2008). "A transcriptome database for astrocytes, neurons, and oligodendrocytes: a new resource for understanding brain development and function." J Neurosci **28**(1): 264-278.

Cannon, C. L., et al. (1998). "Intracellular ionic strength regulates the volume sensitivity of a swelling-activated anion channel." Am J Physiol **275**(2 Pt 1): C416-422.

Cardin, V., et al. (2003). "Potentiation of the osmosensitive taurine release and cell volume regulation by cytosolic Ca2+ rise in cultured cerebellar astrocytes." Glia **44**(2): 119-128.

Carton, I., et al. (2002). "RhoA exerts a permissive effect on volume-regulated anion channels in vascular endothelial cells." Am J Physiol Cell Physiol **283**(1): C115-125.

Cheema, T. A., C. E. Ward, et al. (2005). "Subnanomolar concentrations of thrombin enhance the volume-sensitive efflux of taurine from human 1321N1 astrocytoma cells." J Pharmacol Exp Ther **315**(2): 755-763.

Chvatal, A., M. Anderova, et al. (2007). "Three-dimensional confocal morphometry reveals structural changes in astrocyte morphology in situ." J Neurosci Res 85(2): 260-271.

Crepel, V., et al. (1998). "Mitogen-activated protein and tyrosine kinases in the activation of astrocyte volume-activated chloride current." J Neurosci **18**(4): 1196-1206.

D'Ambrosio, R., et al. (2002). "Differential role of KIR channel and Na(+)/K(+)-pump in the regulation of extracellular K(+) in rat hippocampus." J Neurophysiol **87**(1): 87-102.

Darby, M., J. B. Kuzmiski, et al. (2003). "ATP released from astrocytes during swelling activates chloride channels." J Neurophysiol **89**(4): 1870-1877.

Decher, N., H. J. Lang, et al. (2001). "DCPIB is a novel selective blocker of I(Cl,swell) and prevents swelling-induced shortening of guinea-pig atrial action potential duration." Br J Pharmacol **134**(7): 1467-1479.

Deleuze, C., et al. (1998). "Properties and glial origin of osmotic-dependent release of taurine

from the rat supraoptic nucleus." J Physiol **507 (Pt 2)**: 463-471.

Dietz, R. M., et al. (2007). "Contribution of Na(+)/Ca(2+) exchange to excessive Ca(2+) loading in dendrites and somata of CA1 neurons in acute slice." Hippocampus **17**(11): 1049-1059.

Djukic, B., et al. (2007). "Conditional knock-out of Kir4.1 leads to glial membrane depolarization, inhibition of potassium and glutamate uptake, and enhanced short-term synaptic potentiation." J Neurosci **27**(42): 11354-11365.

Emma, F., et al. (1998). "Effect of cell swelling on membrane and cytoplasmic distribution of pICln." Am J Physiol **274**(6 Pt 1): C1545-1551.

Emma, F., et al. (1997). "Intracellular electrolytes regulate the volume set point of the organic osmolyte/anion channel VSOAC." Am J Physiol **272**(6 Pt 1): C1766-1775.

Estevez, A. Y., M. H. O'Regan, et al. (1999). "Effects of anion channel blockers on hyposmotically induced amino acid release from the in vivo rat cerebral cortex." Neurochem Res **24**(3): 447-452.

Ferroni, S., et al. (1995). "Two distinct inwardly rectifying conductances are expressed in long term dibutyryl-cyclic-AMP treated rat cultured cortical astrocytes." FEBS Lett **367**(3): 319-325.

Feustel, P. J., et al. (2004). "Volume-regulated anion channels are the predominant contributors to release of excitatory amino acids in the ischemic cortical penumbra." Stroke **35**(5): 1164-1168.

Habela, C. W., et al. (2009). "Chloride accumulation drives volume dynamics underlying cell proliferation and migration." J Neurophysiol **101**(2): 750-757.

Hansson, E. and L. Rönnbäck (2003). Astrocytic receptors and second messenger systems. Advances in Molecular and Cell Biology. H. Leif, Elsevier. **Volume 31:** 475-501.

Haskew-Layton, R. E., et al. (2005). "Hydrogen peroxide potentiates volume-sensitive excitatory amino acid release via a mechanism involving Ca2+/calmodulin-dependent protein kinase II." J Biol Chem **280**(5): 3548-3554.

Haskew, R. E., et al. (2002). "Peroxynitrite enhances astrocytic volume-sensitive excitatory amino acid release via a src tyrosine kinase-dependent mechanism." J Neurochem **82**(4): 903-912.

Hermoso, M., et al. (2002). "ClC-3 is a fundamental molecular component of volume-sensitive outwardly rectifying Cl- channels and volume regulation in HeLa cells and Xenopus laevis oocytes." J Biol Chem **277**(42): 40066-40074.

Herrera, J. L., et al. (2011). "Estradiol and tamoxifen differentially regulate a plasmalemmal

voltage-dependent anion channel involved in amyloid-beta induced neurotoxicity." Steroids **76**(9): 840-844.

Higashi, K., et al. (2001). "An inwardly rectifying K(+) channel, Kir4.1, expressed in astrocytes surrounds synapses and blood vessels in brain." Am J Physiol Cell Physiol **281**(3): C922-931.

Hirrlinger, P. G., et al. (2008). "Osmotic swelling characteristics of glial cells in the murine hippocampus, cerebellum, and retina in situ." J Neurochem **105**(4): 1405-1417.

Hisadome, K., et al. (2002). "Volume-regulated anion channels serve as an auto/paracrine nucleotide release pathway in aortic endothelial cells." J Gen Physiol **119**(6): 511-520.

Horgan, K., et al. (1986). "Inhibition of protein kinase C mediated signal transduction by tamoxifen. Importance for antitumour activity." Biochem Pharmacol **35**(24): 4463-4465.

Inoue, H. and Y. Okada (2007). "Roles of volume-sensitive chloride channel in excitotoxic neuronal injury." J Neurosci **27**(6): 1445-1455.

Jackson, P. S., et al. (1994). "The volume-sensitive organic osmolyte-anion channel VSOAC is regulated by nonhydrolytic ATP binding." Am J Physiol **267**(5 Pt 1): C1203-1209.

Jackson, P. S. and K. Strange (1995). "Characterization of the voltage-dependent properties of a volume-sensitive anion conductance." J Gen Physiol **105**(5): 661-676.

Kahle, K. T., J. M. Simard, K. J. Staley, B. V. Nahed, P. S. Jones and D. Sun (2009). "Molecular mechanisms of ischemic cerebral edema: role of electroneutral ion transport." Physiology (Bethesda) 24: 257-265.

Kimelberg, H. K., S. K. Goderie, S. Higman, S. Pang and R. A. Waniewski (1990). "Swelling-induced release of glutamate, aspartate, and taurine from astrocyte cultures." J Neurosci 10(5): 1583-1591.

Kimelberg, H. K. (2004). "Increased release of excitatory amino acids by the actions of ATP and peroxynitrite on volume-regulated anion channels (VRACs) in astrocytes." Neurochem Int **45**(4): 511-519.

Kimelberg, H. K. (2005). "Astrocytic swelling in cerebral ischemia as a possible cause of injury and target for therapy." Glia **50**(4): 389-397.

Kimelberg, H. K., et al. (2004). "Inhibition of release of taurine and excitatory amino acids in ischemia and neuroprotection." Neurochem Res **29**(1): 267-274.

Koizumi, S. (2010). "Synchronization of Ca2+ oscillations: involvement of ATP release in astrocytes." FEBS J **277**(2): 286-292.

Kubo, M. and Y. Okada (1992). "Volume-regulatory Cl- channel currents in cultured human

epithelial cells." J Physiol **456**: 351-371.

Langer, J. and C. R. Rose (2009). "Synaptically induced sodium signals in hippocampal astrocytes in situ." J Physiol **587**(Pt 24): 5859-5877.

Lascola, C. D. and R. P. Kraig (1996). "Whole-cell chloride currents in rat astrocytes accompany changes in cell morphology." J Neurosci **16**(8): 2532-2545.

Lenart, B., et al. (2004). "Na-K-Cl cotransporter-mediated intracellular Na+ accumulation affects Ca2+ signaling in astrocytes in an in vitro ischemic model." J Neurosci **24**(43): 9585-9597.

Lepple-Wienhues, A., et al. (1998). "The tyrosine kinase p56lck mediates activation of swelling-induced chloride channels in lymphocytes." J Cell Biol **141**(1): 281-286.

Liu, H. T., A. H. Toychiev, et al. (2008). "Maxi-anion channel as a candidate pathway for osmosensitive ATP release from mouse astrocytes in primary culture." Cell Res **18**(5): 558-565.

Loaiza, A., et al. (2003). "Glutamate triggers rapid glucose transport stimulation in astrocytes as evidenced by real-time confocal microscopy." J Neurosci **23**(19): 7337-7342.

Lohr, J. W. and J. J. Grantham (1986). "Isovolumetric regulation of isolated S2 proximal tubules in anisotonic media." J Clin Invest **78**(5): 1165-1172.

Maeno, E., et al. (2000). "Normotonic cell shrinkage because of disordered volume regulation is an early prerequisite to apoptosis." Proc Natl Acad Sci U S A **97**(17): 9487-9492.

Maeno, E., N. Takahashi, et al. (2006). "Dysfunction of regulatory volume increase is a key component of apoptosis." FEBS Lett **580**(27): 6513-6517.

Maertens, C., et al. (2002). "Block of volume-regulated anion channels by selective serotonin reuptake inhibitors." Naunyn Schmiedebergs Arch Pharmacol **366**(2): 158-165.

Malarkey, E. B. and V. Parpura (2008). "Mechanisms of glutamate release from astrocytes." Neurochem Int **52**(1-2): 142-154.

Matyash, V. and H. Kettenmann (2010). "Heterogeneity in astrocyte morphology and physiology." Brain Res Rev 63(1-2): 2-10.

Massieu, L., et al. (2004). "Brain amino acids during hyponatremia in vivo: clinical observations and experimental studies." Neurochem Res **29**(1): 73-81.

Mizuno, A., et al. (2003). "Impaired osmotic sensation in mice lacking TRPV4." Am J Physiol Cell Physiol **285**(1): C96-101.

Molleman, A. (2003). Patch clamping : an introductory guide to patch clamp electrophysiology. New York, J. Wiley.

Mongin, A. A. (2007). "Disruption of ionic and cell volume homeostasis in cerebral ischemia:

The perfect storm." Pathophysiology **14**(3-4): 183-193.

Mongin, A. A., et al. (1999). "Volume-dependent taurine release from cultured astrocytes requires permissive [Ca(2+)](i) and calmodulin." Am J Physiol **277**(4 Pt 1): C823-832.

Mongin, A. A. and H. K. Kimelberg (2002). "ATP potently modulates anion channel-mediated excitatory amino acid release from cultured astrocytes." Am J Physiol Cell Physiol **283**(2): C569-578.

Mongin, A. A. and H. K. Kimelberg (2005). "ATP regulates anion channel-mediated organic osmolyte release from cultured rat astrocytes via multiple Ca2+-sensitive mechanisms." Am J Physiol Cell Physiol **288**(1): C204-213.

Morales-Mulia, S., et al. (1998). "Osmotic swelling-induced changes in cytosolic calcium do not affect regulatory volume decrease in rat cultured suspended cerebellar astrocytes." J Neurochem **71**(6): 2330-2338.

Moran, J., et al. (1996). "Changes of actin cytoskeleton during swelling and regulatory volume decrease in cultured astrocytes." Am J Physiol **271**(6 Pt 1): C1901-1907.

Mulligan, S. J. and B. A. MacVicar (2006). "VRACs CARVe a path for novel mechanisms of communication in the CNS." Sci STKE **2006**(357): pe42.

Nase, G., P. J. Helm, et al. (2008). "Water entry into astrocytes during brain edema formation." Glia **56**(8): 895-902.

Nilius, B., et al. (2000). "Myosin light chain phosphorylation-dependent modulation of volume-regulated anion channels in macrovascular endothelium." FEBS Lett **466**(2-3): 346-350.

Oberheim, N. A., T. Takano, et al. (2009). "Uniquely hominid features of adult human astrocytes." J Neurosci **29**(10): 3276-3287.

Ogden, D. (1994). Microelectrode techniques : the Plymouth Workshop handbook. Cambridge, Company of Biologists.

Okada, Y. (1997). "Volume expansion-sensing outward-rectifier Cl- channel: fresh start to the molecular identity and volume sensor." Am J Physiol **273**(3 Pt 1): C755-789.

Okada, Y., et al. (2001). "Receptor-mediated control of regulatory volume decrease (RVD) and apoptotic volume decrease (AVD)." J Physiol **532**(Pt 1): 3-16.

Okada, Y., et al. (2009). "Pathophysiology and puzzles of the volume-sensitive outwardly rectifying anion channel." J Physiol.

Olsen, M. L. and H. Sontheimer (2004). "Mislocalization of Kir channels in malignant glia." Glia **46**(1): 63-73.

Ordaz, B., et al. (2004). "Osmolytes and mechanisms involved in regulatory volume decrease

under conditions of sudden or gradual osmolarity decrease." Neurochem Res **29**(1): 65-72.

Ordaz, B., et al. (2004). "Volume changes and whole cell membrane currents activated during gradual osmolarity decrease in C6 glioma cells: contribution of two types of K+ channels." Am J Physiol Cell Physiol **286**(6): C1399-1409.

Parkerson, K. A. and H. Sontheimer (2004). "Biophysical and pharmacological characterization of hypotonically activated chloride currents in cortical astrocytes." Glia **46**(4): 419-436.

Pasantes-Morales, H., et al. (2002). "Mechanisms counteracting swelling in brain cells during hyponatremia." Arch Med Res **33**(3): 237-244.

Pasantes-Morales, H., et al. (2006). "Tyrosine kinases and osmolyte fluxes during hyposmotic swelling." Acta Physiol (Oxf) **187**(1-2): 93-102.

Pasantes-Morales, H., et al. (1993). "Cell volume regulation in cultured cerebellar granule neurons." J Neurosci Res **34**(2): 219-224.

Pasantes-Morales, H. and S. Morales Mulia (2000). "Influence of calcium on regulatory volume decrease: role of potassium channels." Nephron **86**(4): 414-427.

Pasantes-Morales, H., et al. (1994). "Regulatory volume decrease in cultured astrocytes. II. Permeability pathway to amino acids and polyols." Am J Physiol **266**(1 Pt 1): C172-178.

Perea, G. and A. Araque (2005). "Properties of synaptically evoked astrocyte calcium signal reveal synaptic information processing by astrocytes." J Neurosci **25**(9): 2192-2203.

Perea, G., et al. (2009). "Tripartite synapses: astrocytes process and control synaptic information." Trends Neurosci **32**(8): 421-431.

Phillis, J. W. and M. H. O'Regan (2003). "Characterization of modes of release of amino acids in the ischemic/reperfused rat cerebral cortex." Neurochem Int **43**(4-5): 461-467.

Phillis, J. W., et al. (1996). "Inhibition of tyrosine phosphorylation attenuates amino acid neurotransmitter release from the ischemic/reperfused rat cerebral cortex." Neurosci Lett **207**(3): 151-154.

Phillis, J. W., D. Song, et al. (1997). "Inhibition by anion channel blockers of ischemia-evoked release of excitotoxic and other amino acids from rat cerebral cortex." Brain Res **758**(1-2): 9-16.

Phillis, J. W., D. Song, et al. (1998). "Tamoxifen, a chloride channel blocker, reduces glutamate and aspartate release from the ischemic cerebral cortex." Brain Res **780**(2): 352-355.

Ransom, C. B., et al. (2001). "Volume-activated chloride currents contribute to the resting conductance and invasive migration of human glioma cells." J Neurosci **21**(19): 7674-7683.

Ransom, C. B., et al. (2000). "Activity-dependent extracellular K+ accumulation in rat optic nerve: the role of glial and axonal Na+ pumps." J Physiol **522 Pt 3**: 427-442.

Risher, W. C., et al. (2009). "Real-time passive volume responses of astrocytes to acute osmotic and ischemic stress in cortical slices and in vivo revealed by two-photon microscopy." Glia **57**(2): 207-221.

Rose, C. R. and B. R. Ransom (1996). "Intracellular sodium homeostasis in rat hippocampal astrocytes." J Physiol **491 (Pt 2)**: 291-305.

Rose, C. R., S. G. Waxman and B. R. Ransom (1998). "Effects of glucose deprivation, chemical hypoxia, and simulated ischemia on Na+ homeostasis in rat spinal cord astrocytes." J Neurosci 18(10): 3554-3562.

Rudkouskaya, A., A. Chernoguz, et al. (2008). "Two conventional protein kinase C isoforms, alpha and betaI, are involved in the ATP-induced activation of volume-regulated anion channel and glutamate release in cultured astrocytes." J Neurochem.

Rutledge, E. M., A. A. Mongin, et al. (1999). "Intracellular ATP depletion inhibits swelling-induced D-[3H]aspartate release from primary astrocyte cultures." Brain Res **842**(1): 39-45.

Schipke, C. G., et al. (2008). "Astrocytes discriminate and selectively respond to the activity of a subpopulation of neurons within the barrel cortex." Cereb Cortex **18**(10): 2450-2459.

Schliess, F., et al. (1996). "Calcium-dependent activation of Erk-1 and Erk-2 after hypo-osmotic astrocyte swelling." Biochem J **320 (Pt 1)**: 167-171.

Schools, G. P., et al. (2006). "Development of gap junctions in hippocampal astrocytes: evidence that whole cell electrophysiological phenotype is an intrinsic property of the individual cell." J Neurophysiol **96**(3): 1383-1392.

Seifert, G., et al. (2009). "Analysis of astroglial K+ channel expression in the developing hippocampus reveals a predominant role of the Kir4.1 subunit." J Neurosci **29**(23): 7474-7488.

Shen, M. R., et al. (2000). "Differential expression of volume-regulated anion channels during cell cycle progression of human cervical cancer cells." J Physiol **529 Pt 2**: 385-394.

Shimizu, T., T. Numata, et al. (2004). "A role of reactive oxygen species in apoptotic

activation of volume-sensitive Cl(-) channel." Proc Natl Acad Sci U S A **101**(17): 6770-6773.

Simard, M. and M. Nedergaard (2004). "The neurobiology of glia in the context of water and ion homeostasis." Neuroscience **129**(4): 877-896.

Stobrawa, S. M., et al. (2001). "Disruption of ClC-3, a chloride channel expressed on synaptic vesicles, leads to a loss of the hippocampus." Neuron **29**(1): 185-196.

Ternovsky, V. I., et al. (2004). "Sizing the pore of the volume-sensitive anion channel by differential polymer partitioning." FEBS Lett **576**(3): 433-436.

Tilly, B. C., et al. (1993). "Protein tyrosine phosphorylation is involved in osmoregulation of ionic conductances." J Biol Chem **268**(27): 19919-19922.

Tominaga, M., et al. (1995). "Volume-sensitive chloride channel activity does not depend on endogenous P-glycoprotein." J Biol Chem **270**(46): 27887-27893.

Valverde, M. A., et al. (1992). "Volume-regulated chloride channels associated with the human multidrug-resistance P-glycoprotein." Nature **355**(6363): 830-833.

Van der Wijk, T., et al. (1999). "Osmotic cell swelling-induced ATP release mediates the activation of extracellular signal-regulated protein kinase (Erk)-1/2 but not the activation of osmo-sensitive anion channels." Biochem J **343 Pt 3**: 579-586.

Ventura, R. and K. M. Harris (1999). "Three-dimensional relationships between hippocampal synapses and astrocytes." J Neurosci **19**(16): 6897-6906.

Verkhratsky, A. N. and A. Butt (2007). Glial neurobiology : a textbook. Chichester, England a; Hoboken, NJ, John Wiley & Sons.

Voets, T., et al. (1996). "The chloride current induced by expression of the protein pICln in Xenopus oocytes differs from the endogenous volume-sensitive chloride current." J Physiol **495 (Pt 2)**: 441-447.

Voets, T., et al. (1999). "Reduced intracellular ionic strength as the initial trigger for activation of endothelial volume-regulated anion channels." Proc Natl Acad Sci U S A **96**(9): 5298-5303.

Walz, W. and M. K. Lang (1998). "Immunocytochemical evidence for a distinct GFAP-negative subpopulation of astrocytes in the adult rat hippocampus." Neurosci Lett **257**(3): 127-130.

Wang, Y., et al. (1996). "Autocrine signaling through ATP release represents a novel mechanism for cell volume regulation." Proc Natl Acad Sci U S A **93**(21): 12020-12025.

Wegierski, T., U. Lewandrowski, et al. (2009). "Tyrosine phosphorylation modulates the

activity of TRPV4 in response to defined stimuli." J Biol Chem **284**(5): 2923-2933.

Wilhelmsson, U., E. A. Bushong, et al. (2006). "Redefining the concept of reactive astrocytes as cells that remain within their unique domains upon reaction to injury." Proc Natl Acad Sci U S A **103**(46): 17513-17518.

Ye, Z. C., N. Oberheim, H. Kettenmann and B. R. Ransom (2009). "Pharmacological "cross-inhibition" of connexin hemichannels and swelling activated anion channels." Glia 57(3): 258-269.

Zhang, H., et al. (2011). "Volume regulated anion channel currents of rat hippocampal neurons and their contribution to oxygen-and-glucose deprivation induced neuronal death." PLoS One **6**(2): e16803.

Zhang, Y., et al. (2008). "DCPIB, a specific inhibitor of volume regulated anion channels (VRACs), reduces infarct size in MCAo and the release of glutamate in the ischemic cortical penumbra." Exp Neurol **210**(2): 514-520.

Zhou, M., et al. (2006). "Development of GLAST(+) astrocytes and NG2(+) glia in rat hippocampus CA1: mature astrocytes are electrophysiologically passive." J Neurophysiol **95**(1): 134-143.

Zhou, M., et al. (2009). "TWIK-1 and TREK-1 are potassium channels contributing significantly to astrocyte passive conductance in rat hippocampal slices." J Neurosci **29**(26): 8551-8564.